research articles Journal of proteome research

Global Analysis of Quorum Sensing Targets in the Intracellular Pathogen *Brucella melitensis* 16 M

Sophie Uzureau,[†,‡,§] Julien Lemaire,[†,§] Edouard Delaive,[||] Marc Dieu,[||] Anthoula Gaigneaux,[†] Martine Raes,[||] Xavier De Bolle,[†] and Jean-Jacques Letesson*[,†]

Unité de Recherche en Biologie Moléculaire, Laboratoire d'Immunologie-Microbiologie, FUNDP - University of Namur, Namur, Belgium, Unité de Recherche en Biologie Cellulaire, FUNDP - University of Namur, Namur, Belgium, and Laboratoire de Parasitologie Moléculaire, Université Libre de Bruxelles, Gosselies, Belgium

Received January 25, 2010

Many pathogenic bacteria use a regulatory process termed quorum sensing (QS) to produce and detect small diffusible molecules to synchronize gene expression within a population. In Gram-negative bacteria, the detection of, and response to, these molecules depends on transcriptional regulators belonging to the LuxR family. Such a system has been discovered in the intracellular pathogen *Brucella melitensis*, a Gram-negative bacterium responsible for brucellosis, a worldwide zoonosis that remains a serious public health concern in countries were the disease is endemic. Genes encoding two LuxR-type regulators, VjbR and BabR, have been identified in the genome of *B. melitensis* 16 M. A Δ*vjbR* mutant is highly attenuated in all experimental models of infection tested, suggesting a crucial role for QS in the virulence of *Brucella*. At present, no function has been attributed to BabR. The experiments described in this report indicate that 5% of the genes in the *B. melitensis* 16 M genome are regulated by VjbR and/or BabR, suggesting that QS is a global regulatory system in this bacterium. The overlap between BabR and VjbR targets suggest a cross-talk between these two regulators. Our results also demonstrate that VjbR and BabR regulate many genes and/or proteins involved in stress response, metabolism, and virulence, including those potentially involved in the adaptation of *Brucella* to the oxidative, pH, and nutritional stresses encountered within the host. These findings highlight the involvement of QS as a major regulatory system in *Brucella* and lead us to suggest that this regulatory system could participate in the spatial and sequential adaptation of *Brucella* strains to the host environment.

Keywords: *Brucella* • intracellular pathogen • Quorum sensing • LuxR-type regulator • adaptation • proteome • transcriptome • ChIP

Introduction

Bacteria of the genus *Brucella* are the etiological agents of brucellosis, the most widespread zoonotic disease worldwide, resulting in more than 500 000 new reported human cases per year.[1] Animal brucellosis is a disease affecting wild and domestic animals, causing abortion and sterility and producing huge economic losses.[2] Several of the nine *Brucella* species can infect humans, causing a chronic, debilitating disease with severe and sometimes fatal outcomes. As a result, these bacteria represent a significant public health concern in endemic countries (predominantly in the Mediterranean region and areas of Asia, Africa and Latin America).[1,3] Because of their potential use as weapons, *B. melitensis*, *B. suis* and *B. abortus* strains have been classified as select agents by the Center for Disease Control and Prevention in the U.S.A.[4]

Brucella strains are Gram-negative intracellular pathogens belonging to the α-2 proteobacteria group. The virulence of these bacteria is based on their capacity to infect professional and nonprofessional phagocytes.[5−8] This remarkable adaptation to the intracellular environment and their ability to modulate the host innate immune response[9] allows the *Brucellae* to establish and maintain chronic infections. During host cell infection, *Brucella* containing vacuoles (BCVs) traffic along the endocytic pathway and fuse transiently with both late endosomes and lysosomes, and such interactions are required for further maturation of BCVs into an ER-derived replication-permissive organelle.[10] The virulence strategies of these bacteria seem to be based on poor stimulatory activity and toxicity for host cells,[9] resistance to intracellular killing,[11] adaptation to intracellular stresses[12,13] and creation of the replication-permissive compartment in professional and nonprofessional phagocytes.[8,14]

* To whom correspondence should be addressed. Mailing address: FUNDP - University of Namur, Namur, Belgium, Unité de Recherche en Biologie Moléculaire, Laboratoire d'Immunologie-Microbiologie, rue de Bruxelles 61, 5000-Namur, Belgium. Phone: (32) 81 72 44 02. Fax: (32) 81 72 42 97. E-mail: jean-jacques.letesson@fundp.ac.be.

† Unité de Recherche en Biologie Moléculaire, FUNDP - University of Namur.

‡ Université Libre de Bruxelles.

§ These authors contributed equally to this work.

|| Unité de Recherche en Biologie Cellulaire, FUNDP - University of Namur.

10.1021/pr100068p

Published on Web 04/13/2010

During infection, *Brucella* spp. are confronted with very diverse environments and host defense mechanisms.[12,15−17] Thus, completion of a successful infection cycle is crucially dependent on fine-tuning gene expression in response to environmental stimuli.[18] Among the systems that allow such regulations, quorum sensing (QS) is of particular interest because of its documented involvement in the virulence of *Brucella*[19] and other pathogens.[20,21] QS is a communication system used by a large number of bacteria to synchronize gene expression within a population. This system involves the synthesis, release and subsequent detection of small diffusible molecules called autoinducers (commonly *N*-acyl-homoserine lactones or AHLs in Gram-negatives bacteria). When AHL concentrations reach a threshold level, they bind to LuxR-type transcriptional regulators and modify their activity (for review see ref 22). Since QS was first discovered in *V. fischeri* in the late 1970s,[23] the conceptual role of this communication system in prokaryotic biology has evolved considerably. QS was first described as a system allowing bacteria to sense population density.[24] However, the autoinducer concentrations can be affected by numerous parameters like diffusion, spatial distribution, and degradation.[25,26] These latter factors are particularly relevant given the intravacuolar localization of *Brucella* spp. in host cells.

Genes encoding two LuxR-type regulators have been identified in the *B. melitensis* 16 M genome,[27] the previously described VjbR regulator[19,28] and BabR,[29] also known as BlxR.[30] While the virulence of a Δ*vjbR* strain is highly attenuated in all experimental model tested, BabR seems *to* play a minor, if any role, in *B. melitensis* 16 M virulence.[31] Despite the lack of a gene encoding a classical AHL synthase in the genome of *B. melitensis*, we have previously identified low amounts of C_{12}−HSL in culture supernatants from these strains.[32] This autoinducer down-regulates the expression of flagellar genes,[19] and the expression of the *virB* operon encoding a Type four secretion system (T4SS),[32,33] two virulence factors involved in the establishment of chronic infection[34] and the control of *Brucella* containing vacuole (BCV) maturation, respectively.[35] Experimental evidence suggests that VjbR mediates the effect of C_{12}−HSL on *virB* transcription[28] by binding to a 18 bp palindromic motif in the *virB* promoter.[36] Moreover it was recently demonstrated that VjbR is involved in the regulation of exopolysaccharide (EPS) synthesis and/or export and the production of several outer membrane proteins (OMPs), some of which are involved in virulence, suggesting that this regulator plays a crucial role in the regulation of the surface properties of *B. melitensis* 16 M.[28]

The work described in this paper is the first attempt to identify the QS regulon of an intracellular pathogen. To accomplish this, we characterized Δ*babR* and Δ*vjbR* mutants by 2D-DIGE and microarray analysis on the same samples. We identified 101 QS targets using the proteomic approach and 338 QS target genes by transcriptome analysis. To focus on the most confident targets, we focus only on those that were identified by both proteomic and microarray analysis and those from the microarray analysis that were confirmed by qRT-PCR, chromatin immunoprecipitation (chIP) or other biological validation experiments. This combinatorial screen allowed us to select 149 VjbR and BabR target genes representing 4.7% of the *B. melitensis* 16 M genome. Interestingly many of these targets were regulated by both VjbR and BabR, suggesting a cross-talk between these two LuxR type regulators. Our analysis revealed that the QS system of this intracellular bacterium is a global regulatory system because VjbR and BabR control (directly or not) genes and proteins involved in stress response, metabolic adaptation and virulence. In the light of these results, we therefore propose that the *B. melitensis* QS system may play a role in fine-tuning the spatiotemporal adaptation of the bacteria to their intracellular niche.

Experimental section

Bacterial Strains and Culture Conditions. *Brucella melitensis* strains were grown with shaking at 37 °C in 2YT medium (10% yeast extract, 10 g L^{-1} tryptone, 5 g L^{-1} NaCl) containing the appropriate antibiotics, from an initial optical density at 600 nm (OD_{600}) of 0.05. For transcriptomic and proteomic analyses, 100 mL of 2YT without antibiotic were inoculated with wild-type strain, Δ*vjbR* or Δ*babR* mutants to an OD_{600} of 0.05. Cultures were grown in triplicate, and incubated at 37 °C with shaking to an OD_{600} of 0.75. Ten milliliters of culture was used for protein preparation, and the rest was used for RNA extraction.

Nalidixic acid (Nal) and gentamycin (Gnt) were used at 25 μg mL^{-1} and 50 μg mL^{-1} respectively. Synthetic *N*-dodecanoyl-DL-homoserine lactone (C_{12}−HSL; Fluka) was prepared in acetonitrile (ACN) and added to bacterial growth media at 5 μM final concentration. The same volume of ACN was used as a negative control.

Mutant Construction. The Δ*babR* and Δ*vjbR* mutant strains were constructed by gene replacement employing a kanamycine resistance gene and previously described procedures.[19,31]

For ChIP experiments, the plasmid pSB502 harboring a C-terminal fusion between the flag tag and the $vjbR_{HTH}$ region coding for the HTH region of VjbR (amino acids 181 to 260) was designed as following. First, we constructed the Gateway destination vector pSB500 allowing C-terminal fusions of an ORF with the flag epitope under P*lac* control. The Gw-Flag cassette was excised from the pGEMT-Gw-FLAG Cter (from Geraldine Laloux) by an *Apa*I/*Sac*I restriction. The resulting fragment was purified and ligated in the pBBR1MCS-5[37] plasmid restricted by the same enzymes to obtain the destination vector pSB500 (containing a Gnt resistance cassette). The entry clone pSB102 containing $vjbR_{HTH}$[28] was used together with the destination vector pSB500 during Gateway LR reaction as described by Dricot and co-workers.[38] The resulting vector pSB502 and the pBBRmcs-5 plasmid (negative control) were introduced in *Brucella melitensis* Δ*vjbR* strain by mating.

Matings were performed by mixing 200 μL of *E. coli* S17−1 donor cells liquid culture (overnight culture) and 1 mL of the *B. melitensis* Nal^R recipient strain (overnight culture). Cells were centrifuged 2 min at 7000 rpm and washed two times with 2YT. The pellets were resuspended in 10 μL of 2YT and spotted on a 2YT plate for 4 h. Bacteria were then transferred onto a 2YT plate containing Gnt and Nal. After 3 days of incubation at 37 °C, the exconjugates were replicated on a 2YT plate containing Nal and Gnt.

Microarray Experiments. RNA Preparation. Total RNA was extracted from *B. melitensis* 16 M and the isogenic Δ*vjbR* and Δ*babR* mutants (all cultured in triplicate) as follows: 45 mL of culture (OD_{600} of 0.75) were centrifuged at 3500 rpm for 15 min. Bacterial pellets were resuspended in 100 μL SDS 10% and 20 μL proteinase K (20 mg mL^{-1}) and incubated at 37 °C with shaking for 1 h. Five milliliters of TRIzol Reagent (Invitrogen) were added and suspensions were vigorously shacken. After 10 min of incubation at 65 °C, 1 mL chloroform was added to the suspensions and the mixtures were shacken and incubated

at room temperature for 5−10 min. Samples were then centrifuged at 14.000 rpm for 15 min at 4 °C. Then, 2.5 mL 2-propanol were added to the aqueous phases and samples were stored overnight at −20 °C. After centrifugation for 30 min at 14.000 rpm at 4 °C, pellets were washed with 75% (RNase free) ethanol. Supernatants were discarded and pellets were dried 15 min at room temperature. Total RNA samples were resuspended in 100 μL RNase free water, incubated 10 min at 55 °C and stored at −80 °C. The integrity of the RNA and the absence of DNA were checked by gel electrophoresis. RNA quantity was measured using a NanoDrop spectrophotometer (ND-1000, Thermo Fisher Scientific).

Microarray Analysis. Microarray design and analysis were made by NimbleGen Systems, Inc. from catalogue design for *B. melitensis* 16 M chromosomes I (NC_003317) and II (NC_003318) with 20 probes per gene (10 perfect matches and 10 mismatches). Each probe (24 mer) was replicated three times on a chip (design includes random GC probes). Triplicate RNA samples of each strain were mixed and one chip was analyzed per strain. The data discussed in this publication have been deposited in NCBI's Gene Expression Omnibus and are accessible for reviewers through GEO Series accession number GSE8844 (http://www.ncbi.nlm.nih.gov/geo/query/acc.cgi?token=jzmhfuoccmeugfi&acc=GSE8844).

All of the analysis was performed using the statistical program in the *stats* package.[39] Data obtained from the microarray analysis were preprocessed using the RMA algorithm,[40] as provided by NimbleGen Systems, Inc. Two pair wise comparisons were performed (Δ*vjbr* vs wt) and (Δ*babr* vs wt). For each comparison, the fold change was computed as the ratio of intensity averages (mutant/wt). A Student *t* test was used for statistical analysis of overexpression and underexpression. Genes presenting both a fold change greater than 1.3 (or below 0.7) and statistical significance at the alpha level 0.005 were defined as being over- or under-expressed between the two strains being compared.

Two-Dimensional Difference in Gel Electrophoresis (2D-DIGE). Samples Preparation and Electrophoresis. Proteins were extracted from 10 mL of *B. melitensis* 16 M and Δ*vjbR* and Δ*babR* cultures (OD_{600} 0.75) in triplicate. Cultures were centrifuged at 3500 rpm for 10 min. Bacterial pellets were washed three times with 20 mL PBS before resuspension in 2 mL chloroform. The mixtures were incubated at room temperature for 1 h and then centrifuged at 3500 rpm for 10 min at 4 °C. Pellets were resuspended in PBS to obtain an OD_{600} of 100 and the cell suspensions subjected to three freeze/thaw cycles. Protein concentration for the cell lysates were determined using the BCA Protein Assay (Pierce) and protein concentrations were adjusted to 5−10 μg μL^{-1}. Samples were divided into 100 μg aliquots and one volume of 10% trichloroacetic acid (TCA) was added. The mixtures incubated for 5 min on ice and centrifuged at 14 000 rpm for 3 min at 4 °C. Pellets were resuspended in one volume of 5% TCA and the mixes were incubated 5 min on ice. Samples were centrifuged at 14 000 rpm for 3 min at 4 °C and pellets were washed with ice cold acetone. After centrifugation an additional centrifugation step, pellets were resuspended in a mix of 40 μL Buffer 1 (40 μM Tris HCl pH 8.5, 0.3% SDS) and 4 μL Buffer 2 (0.4 M Tris HCl pH 8.5, 1 mg mL^{-1} DNaseI, 0.25 mg mL^{-1} RNase A; 50 mM $MgCl_2$).

We used the 2D-DIGE method to compare total protein extracts from wt and Δ*vjbR* strains and from wt and Δ*babR* strains. For each comparison, two types of gels (pH 4−7 and pH 7−11 NL) were run in triplicate. Proteins were labeled with CyDye DIGE Fluor, minimal dyes (GE Healthcare) according to the manufacturer, which allows the detection of two prelabeled protein samples and an internal standard on the same 2-D electrophoresis gel. Two samples of 25 μg (wt and Δ*vjbR* or wt and Δ*babR*) were labeled with Cy3 and Cy5, respectively, and analyzed on the same gel together with an internal standard labeled with Cy2 (25 μg). The internal standard was a pool that included an equal amount of proteins of all samples run on triplicate gels. Labeled proteins were first separated by isoelectric focusing in immobilized pH gradient (IPG) gels, linear pH 4−7 gradient or nonlinear pH 7−11 gradient, using IPGphor (GE Healthcare). IPG pH 4−7 gels were run for 3 h at 300 V, 6 h at 1000 V, 3 h at 8000 V and 50 000 Vh at 8000 V and nonlinear IPG pH 7−11 gels were run for 4 h at 500 V, 7 h at 1000 V, 3 h at 8000 V and 60 000 Vh at 8000 V. First-dimension gels were laid on the top of 10% polyacrylamide gels and run using the Ettan Dalt II System (GE Healthcare) at constant 1.5W per gel for 18 h overnight at 15 °C. Gels were scanned with the Typhoon 9600 laser scanner (GE Healthcare) and images were analyzed with the DeCyder Differential Analysis Software (GE Healthcare).

The differential in-gel analysis mode of the DeCyder software was used to merge the Cy2, Cy3, and Cy5 images for each gel, to detect spot limits for the calculation of normalized spot volumes/protein abundances and to determine abundance differences between samples run on the same gel. The biological variation analysis mode of DeCyder was then used to match all pairwise image comparisons from difference in-gel analyses for a comparative cross-gel statistical analysis. Comparison of normalized Cy3 and Cy5 spot volumes with the corresponding Cy2 standard spot volumes within each gel gave a standardized abundance. This value was compared across all gels for each matched spot and a statistical analysis was performed. The Biological Variation Analysis (BVA) provides the average ratios between *B. melitensis* 16 M and mutated strain, with a threshold at ±1.3 and a *t* test confidence of ≤0.05, generating a list of spots of interest. All selected spots were picked, digested and identified using LC−MS/MS.

Mass Spectrometry and Protein Identification. To identify selected spots, preparative gels including 300 μg of proteins (from *B. melitensis* 16 M, Δ*vjbR* and Δ*babR* triplicate samples) were performed following the protocol described above except that they were post stained with ruthenium(II) tris(bathophenanthroline disulfonate) overnight (7 μL of ruthenium/1 L of 20% ethanol) after 6 h of fixation in 30% ethanol, 10% acetic acid and 3 × 30 min in 20% ethanol at 20 °C.[41]

Protein spots were excised from preparative gels by using the Ettan Spot Picker (GE Healthcare) and in-gel tryptic digestion performed as previously described.[42] The gel pieces were twice washed with distilled water and then treated with 100% acetonitrile. The proteolytic digestion was performed by the addition of 3 μL of modified trypsin (Promega) suspended in 50 mM NH_4HCO_3 cold buffer. Proteolysis was performed overnight at 37 °C. The supernatant was collected and combined with the eluate of a subsequent elution step with 5% formic acid.

MALDI-TOF Identification. Digested peptides digest were desalted using C18 Geloader pipet Tips (Proxeon Biosystems) and directly eluted on the target with a mix (1:1 v/v) of α-cyano-4-hydroxyciannamic acid (in 7:3 v/v acetonitrile/0.1% formic acid) and 2,5-dihydroxybenzoic acid (in 7:3 v/v acetonitrile/0.1% trifluoracetic acid). Peptide mass fingerprints were ob-

tained using a MALDI-MX mass spectrometer (Waters, Mildorf, U.S.A.) piloted with MassLynx 4.0 software (Waters). ProteinLynx Global Server 2.2.5 (Waters) was used as the peaklist generating software. MALDI calibration was done with ADH digest and two lockmass calibrations were used. First, an external lockmass with ADH digest (m/z: 1618.84 Da) and finally we applied an internal lockmass based on the trypsin autodigestion peak at 2211.1046 Da. The background subtract threshold was fixed at 15% (polynomial 5, we combined all spectra). An in house Mascot 2.2 server was used as database search engine, PMF search was performed on the Proteobacteria subset of the National Center for Biotechnology Information nonredundant database (NCBInr; 1 391 518 sequences in October 2008). Parameters for peptide matching were a peptide tolerance of 100 ppm, a maximum of one missed cleavage, carbamidomethylation was allowed as a fixed modification and oxidation of methionine was allowed as a variable modification. For all protein identifications, a minimal individual score of 73 and expected value below 1 were used for the identification criteria. All MS/MS spectra can be found in the Supporting Information.

Q-TOF Identification. The digests were separated by reverse phase liquid chromatography using a 75 μm × 150 mm reverse phase NanoEase column (Waters) in a CapLC (Waters) liquid chromatography system. Q-TOF2 and CapLC systems were piloted by MassLynx 4.0 (Waters). Peak lists were created using Mascot Distiller 2.2 (Matrix Science). Enzyme specificity was set to trypsin and the maximum number of missed cleavages per peptide was set at 1. Carbamidomethylation was allowed as a fixed modification and oxidation of methionine was allowed as a variable modification. Mass tolerance for the monoisotopic precursor peptide window was set to 100 ppm and MS/MS tolerance window to ±0.3 Da. We also specified ESI-Q-TOF as the instrument. The peak lists were searched against the Proteobacteria subset of the National Center for Biotechnology Information nonredundant database (NCBInr; 1 391 518 sequences in October 2008). For all protein identifications, a minimal individual ions score of 45 (identity score) and expected value below 1 were used for the initial identification criteria. In the case of redundant protein identifications, the protein identification with the highest score was selected. Moreover, the correlation between theoretical pI and molecular mass of the protein with the position of the corresponding spot in the 2D gel was also taken into account. All MS/MS spectra can be found in the Supporting Information.

Quantitative Real-Time RT-PCR. Total RNA samples were prepared as described above on *B. melitensis* 16 M wild-type strain grown in 2YT with 5 μM final concentration C_{12}−HSL or ACN at 37 °C with shaking to an OD_{600} of 0.75. DNA was removed from the samples using the DNA-free kit (Ambion) and reverse-transcription performed with SuperScript II Reverse Transcriptase (Invitrogen). cDNA samples were used as template in real-time PCR reactions. Primers were designed with the PrimerExpress 2.0 (Applied Biosystems; sequences are listed in Table 3, Supporting Information), PCR products ranged from 80 to 100 bp. Real-time PCR reactions were performed with SYBR Green Mix (Applied Biosystems) in 96-well Optical Reaction plates (Applied Biosystems). Ratios were calculated using the ΔΔCT method for each primer in an Applied Biosystems Step One Plus real-time PCR instrument. Results for each target mRNA was normalized to BMEI0861 mRNA and averaged.

Chromatin Immunoprecipitation Assay. Δ*vjbR* pSB502 (encoding $vjbR_{HTH}$C-terminal flag fusion) and Δ*vjbR* pBBR1MCS-5 (negative control) strains were grown in 2YT at 37 °C to an OD_{600} of 0.75. ChIP experiments were performed essentially as described[43] using antiflag m2 monoclonal antibodies (Sigma). Briefly, after bacterial growth, formaldehyde (1%) was added to 10 mL of triplicate cultures and the cultures placed at room temperature for 10 min before quenching the reaction with glycine (125 mM) for 5 min. Bacteria were collected and washed with cold phosphate-buffered saline twice. The cells were lysed in 0.9 mL of lysis solution (10 mM Tris pH 8.0, 50 mM NaCl, 10 mM EDTA, 20% sucrose, 20 mg mL^{-1} lysozyme) and 0.9 mL of 2× RIPA solution (100 mM Tris pH 8.0, 300 mM NaCl, 2% Nonidet P-40, 1% sodium deoxycholate, 0.2% SDS). The cell extracts were sonicated to fragment DNA to an average size of 500 bp and centrifuged 30 min at 13 000 rpm 4 °C, supernatants were stored at −80 °C. Fifteen μL of the extract was removed for total DNA preparation. For immunoprecipitation of VjbR cross-linked DNA, a portion of the extracts (500 μL) was first cleared with 80 μL of Sepharose-Protein G beads (Sigma) for 1 h at 4 °C and then incubated with 4 μL of monoclonal antiflag m2 antibodies (Sigma) for 4 h at 4 °C. The beads were washed twice with 1× RIPA solution, then twice with LiCl/detergent solution (10 mM Tris pH 8.0, 250 mM LiCl, 1 mM EDTA, 0.5% Nonidet P-40, 0.5% sodium deoxycholate), and finally with TE buffer. The immunoprecipitated material was eluted with 130 μL of elution buffer (25 mM Tris pH 8.0, 5 mM EDTA, 0.5% SDS) for 20 min at 65 °C. Cross-linking of immunoprecipitated and total DNA was reversed by incubation at 65 °C overnight. After Pronase treatment, the immunoprecipitated and total DNA were purified using the PCRapace Kit (Invitek GmbH, Germany) according to the manufacturer.

Analysis of the immunoprecipitated DNA was performed using quantitative PCR with input and immunoprecipitated DNA samples as templates. All promoter-specific primers were designed with Primer Express 1.0 (Applied Biosystems, see supplementary Figure 3) for amplicon sizes and primer localization and sequences). PCR products ranged from 80 to 100 bp. Real-time PCR reactions were performed in 25 μL SYBR Green Mix (Applied Biosystems) in 96-well Optical Reaction plates (Applied Biosystems). Relative quantification using a standard curve method was performed for each primer in an Applied Biosystems 7900HT real-time PCR instrument (absolute quantification method). Input DNA values were used to normalize ChIP, which are presented as a percentage of precipitated DNA (IP)/total DNA (IN).

Assessment of *B. melitensis* Stress Responses. Alkaline and Acid Resistance. *B. melitensis* 16 M and isogenic Δ*vjbR* and Δ*babR* strains were grown in 2YT up to an OD_{600} of 1.0 and diluted to an OD_{600} of 0.05 in 2YT adjusted to the required pH with HCl or NaOH. Cultures were incubated at 37 °C with shaking for 72 h, and OD_{600} were measured after 24, 48, and 72 h of incubation.

Resistance to Bile Salts. In vitro resistance of *B. melitensis* 16 M and the Δ*vjbR* and Δ*babR* strains to bile salts was evaluated as follows. The wt, Δ*vjbR* and Δ*babR* strains were grown in 2YT up to an OD_{600} of 1.0 and were diluted to an OD_{600} 0.05 in 2YT or in 2YT containing 0.1% bile salts (Fluka). Cultures were then incubated at 37 °C with shaking for 18 h and serial dilutions were plated on 2YT medium for CFU counting.

Results and Discussion

Proteomic Analysis of Brucella QS Mutants. To define the QS regulon of *B. melitensis* 16 M, we compared both QS mutants (Δ*vjbR* and Δ*babR*) to the parental (wt) strain by proteomic analysis. Knowing that VjbR, BabR and several virulence factors are expressed during midexponential growth phase, total proteins were extracted under these conditions. 2D-DIGE was then used to compare total protein extracts from three independent midexponential phase cultures of *B. melitensis* 16 M and isogenic Δ*vjbR* and Δ*babR* mutants. For each comparison, two types of gels (pH 4−7 and pH 7−11 NL) were run. Two samples (wt/Δ*vjbR* or wt/Δ*babR*) labeled with Cy3 and Cy5 respectively, were analyzed on the same gel, together with an internal standard labeled with Cy2 (see Material and Methods section). We defined a protein as being affected by the mutation of VjbR or BabR if a difference in abundance of a least 30% compared to the wt strain (Student *t* test $p <$ of 0.05) was observed for that protein in all three gels (one gel for each independent culture). Selected proteins spots corresponding to the 101 different proteins listed in Table 1 were picked, digested and identified using LC−MS/MS. The production of 35 of these proteins is directly or indirectly regulated by VjbR and 66 by BabR. Interestingly, numerous identified proteins are predicted to be involved in metabolic pathways such as central metabolism or amino acid metabolism, respiration, transport of amino acids, sugars and other molecules, secretion and translation.

Transcriptomic Analysis of Brucella QS Mutants. We chose to combine our 2D-DIGE analysis with a transcriptomic study of both QS mutants. Total RNA samples taken at the proteomic analysis step (from the same cultures) were used to maximize the correlation between these two complementary approaches. RNA samples were pooled, retro-transcribed and labeled before hybridization to a *B. melitensis* DNA microarray (Nimblegen).

The gene expression pattern of the Δ*vjbR* strain was compared to profiles generated from the *B. melitensis* 16 M strain. This analysis led to the identification of 296 coding sequences (CDS) (9.2% of the genome) differentially expressed in the *vjbR* mutant strain (see Supplementary Table 1, Supporting Information). Contrary to what was expected based on previous experiments examining the expression of the *virB* and *fliF* promoters,[19] a subset of the predicted VjbR regulon is overexpressed in the mutant strain.

The gene expression pattern of the Δ*babR* strain was compared to profiles generated from the parental strain and revealed that BabR regulated the expression of 42 CDS in *B. melitensis* 16 M (1.3% of the genome, see Supplementary Table 1, Supporting Information).

Our analysis reveals that the regulation of a significant fraction of the *B. melitensis* 16 M genome is influenced by a mutation affecting the QS system. This is consistent with the proposition that QS could act as a global regulatory system in this intracellular pathogen. Similar observations have been previously made in *Escherichia coli*[44] and in the opportunistic pathogen *Pseudomonas aeruginosa*.[45−47] However, we suspect that LuxR-type regulators may directly control only for a fraction of the identified target genes since the expression of genes encoding several transcriptional or post-transcriptional regulators is affected by the Δ*vjbR* and/or the Δ*babR* mutations as can be seen Table 2F.

Notably, several previously known VjbR-regulated genes were identified in this transcriptomic study, (e.g., *virB* and *omp* genes) thus providing an "a priori" validation for the use of the microarray analysis.

Validation of Transcriptional Profiling Results by qRT-PCR. To further validate the results collected from the microarray analysis, we performed a reverse transcription experiment followed by quantitative PCR (qRT-PCR) on RNA samples prepared at exponential growth phase (same $OD_{600\ nm}$ as the transcriptomic experiments but harvested from new cultures). Total RNA was extracted from *B. melitensis* 16 M and isogenic Δ*vjbR* and Δ*babR* mutants. We selected 29 CDS of particular interest (including CDS putatively involved in stress response, virulence and central metabolism) for this analysis. As shown in Table 2, for all the genes tested, the fold changes in transcription detected by qRT-PCR are similar to the fold changes detected by the microarray analysis. A negative control used for each qRT-PCR reaction showed that no genomic DNA contamination occurred in the RNA samples (data not shown).

Selection of the Most Confident *B. melitensis* QS Targets. We used both proteomic and transcriptomic analyses of *vjbR* and *babR* mutants to define the QS regulon of *B. melitensis* 16 M. In order to select the most confident targets, the results obtained with these two complementary methods were combined with previous data on genes regulated by VjbR and BabR.[19,28,36] As the proteomic analysis was performed on three independent samples whereas the transcriptomic one was done on a pool of the corresponding RNA samples, we first based our selection on targets identified by the 2D-DIGE analysis ($n = 99$). We then added to the list CDS identified in the transcriptomic analysis only if they have been confirmed by qRT-PCR ($n = 29$), ChIP ($n = 8$) or a previous biological validation ($n = 14$). Finally, we added CDS predicted to belong to the same transcriptional unit as one of the above selected CDS ($n = 38$). Using this combinatorial analysis, we got a selection of 149 genes whose expression or the amount of gene products formed is affected (directly or indirectly) by VjbR and/or BabR, they are listed in Table 2.

Connections between the Two Brucella QS-Regulators. Analysis of the combined data led to the observation that 27 targets are regulated by both BabR and VjbR (Table 3). The two regulators act in an opposite way on 55% of the genes, including the *virB* genes, and genes encoding chaperones and transporters. These results strongly suggest a crosstalk between the two QS-regulators of *Brucella.* Two recent studies demonstrate that VjbR activates its own expression.[30,36] One of these studies demonstrated a positive regulatory effects of both QS regulators on their own genes as well as the gene encoding the other regulator.[30] However, our transcriptomic analysis revealed that VjbR has a 2-fold activating effect on *babR* expression whereas BabR has a 1.5-fold repressing effect on *vjbR* (Table 2). This observation was confirmed by two different qRT-PCR experiments performed on RNA samples harvested from new cultures (Table 2 and Table 4).

A recent study by Rambow-Larsen and collaborators identified 36 BabR (that they called BlxR) target genes based on a microarray analysis restricted to 289 genes selected for their potential involvement in virulence.[30] Among these 36 targets, only 8 were common to our analysis (8 genes encoding VirB proteins). Strikingly, whereas these genes appeared to be activated by BabR in the study of Rambow-Larsen, they appeared to be repressed in our analysis. These discrepancies could be in part explained by the differences in the experimental design of these two experiments (growth phase, culture medium, and microarray design).

Table 1. Targets Identified by 2D-DIGE Analysis[a]

A cellular function	BMEnnnnn	identification	accession no.	F.C.	# peptides	C %	score	method
			Δ*babR*, pH 4−7					
A.A metabolism	BMEI0231	NAD specific glutamate dehydrogensase	AAL51413.1	0.37	2	1	194	Q-TOF
	BMEI0451	2-isopropyl malate synthase	AAL51632.1	0.21	3	5	183	Q-TOF
	BMEI0811	L-serine dehydratase	AAL51992.1	0.66	5	10	267	Q-TOF
	BMEI0979	Glutamine synthase	AAL52160.1	0.30	2	4	125	Q-TOF
	BMEI1620	Ornithine carbamoyltransferase	AAL52801.1	0.64	2	4	99	Q-TOF
	BMEI1638	Glutamate synthase	AAL52819.1	2.21	4	9	267	Q-TOF
	BMEII0371	β-alanine pyruvate transaminase	AAL53613.1	1.78	6	16	412	Q-TOF
	BMEII0559	Aminomethyltransferase	AAL53801.1	1.68	3	7	191	Q-TOF
Carbohydrate metabolism	BMEI0310	Glycéraldehyde 3-phosphate deshydrogenase	AAL51491.1	1.44	3	9	187	Q-TOF
	BMEI1413	GDP-mannose 4,6-dehydratase	AAL52594.1	0.68	7	16	412	Q-TOF
	BMEI1779	Fructokinase	AAL52960.1	1.61	4	13	246	Q-TOF
	BMEII0358	2-dehydro-3-dehydro-phosphogalactonase aldolase	AAL53600.1	1.38	2	10	141	Q-TOF
Cell wall/envelope	BMEI0727	D-alanine-D-alanine ligase A	AAL51908.1	1.71	6	13	376	Q-TOF
Central metabolism	BMEI0138	Succinyl coA synthetase beta chain	AAL51320.1	1.91	8	18	545	Q-TOF
	BMEI0161	Succinate dehydrogenase	AAL51343.1	0.16	5	9	310	Q-TOF
	BMEI0836	Citrate synthase	AAL52017.1	0.56	2	4	120	Q-TOF
	BMEI0851	Enolase	AAL52032.1	1.34	10	20	614	Q-TOF
	BMEII0248	Phosphoglycerate mutase	AAL53489.1	1.74	4	19	228	Q-TOF
	BMEII0511	Phosphogluconate dehydratase	AAL53753.1	0.08	2	3	144	Q-TOF
Lipid metabolism	BMEI0543	Choloylglycine hydrolase	AAL51724.1	0.11	6	13	375	Q-TOF
	BMEI1112	3-oxo-acyl-carrier protein synthase	AAL52293.1	1.65	5	12	327	Q-TOF
	BMEI1196	EnoylCoA hydratase	AAL52377.1	1.51	2	7	113	Q-TOF
	BMEI1512	Enoyl-(acyl-carrier protein) reductase	AAL52693.1	0.74	7	23	453	Q-TOF
Nucleotide metabolism	BMEI1643	*N*-carbamoyl-L-amino acid amidohydrolase	AAL52824.1	1.62	3	7	210	Q-TOF
Other metabolism	BMEI0176	Porphobilinogene deaminase	AAL51358.1	0.13	3	10	203	Q-TOF
	BMEI0219	Malonate semialdehyde dehydrogenase	AAL51401.1	0.51	3	7	184	Q-TOF
	BMEI0712	CBIG protein/precorrin-3B C17-methyltransferase	AAL51893.1	0.08	3	5	231	Q-TOF
	BMEI1588	Carboxynorspermidine dehydrogenase	AAL52769.1	0.72	3	8	204	Q-TOF
Protein synthesis	BMEI0481	LSU Ribosomal Protein L25P	AAL51662.1	0.71	6	21	472	Q-TOF
	BMEI0742	EF-Tu	AAL51923.1	1.98	14	37	1130	Q-TOF
	BMEI1483	50S ribosomal Protein L9	AAL52664.1	0.12	2	9	121	Q-TOF
	BMEI1915	SSU ribosoma protein S1P	AAL53096.1	1.77	2	3	155	Q-TOF
Regulation	BMEI0626	Transriptional regulator GntR familly	AAL51807.1	2.64	2	5	110	Q-TOF
	BMEII0299	IclR family transcriptional regulator	AAL53541.1	0.73	2	7	83	Q-TOF
	BMEII1116	LuxR regulator VjbR	AAL54358.1	0.55	2	9	164	Q-TOF
Replication/ transcription	BMEI0588	DNA repair protein RecN	AAL51769.1	0.21	4	8	344	Q-TOF
	BMEI0749	DNA-directed RNA polymerase beta chain	AAL51930.1	0.30	7	4	458	Q-TOF
	BMEI1823	DNA gyrase B	AAL53004.1	0.60	7	8	417	Q-TOF
Respiration	BMEI0096	Electron transfer flavoprotein beta subunit	AAL51278.1	1.54	6	27	435	Q-TOF
	BMEI0249	ATP Synthase Alpha Chain	AAL51431.1	0.76	5	9	329	Q-TOF
	BMEI0487	ATP synthase beta subunit/ transription termination factor rho	AAL51668.1	1.61	4	11	216	Q-TOF

Table 1. Continued

cellular function	BMEnnnnn	identification	accession no.	F.C.	# peptides	C %	score	method
Stress/chaperone	BMEI0123	Peptidyl-prolyl cis−trans isomerase	AAL51278.1	1.52	7	21	426	Q-TOF
	BMEI0195	ATP-Dependent Clp Protease, ATP-Binding Subunit ClpB	AAL51377.1	0.74	18	20	1275	Q-TOF
	BMEI0613	Protease DO	AAL51794.1	1.66	7	12	465	Q-TOF
	BMEI2002	DnaK	AAL53183.1	1.78	15	22	1049	Q-TOF
	BMEII0401	Thioredoxine	AAL53643.1	1.71	3	9	224	Q-TOF
	BMEII1048	GroEL	AAL54290.1	0.63	21	48	1727	Q-TOF
Transport/secretion	BMEI1716	Trehalose maltose Binding Protein	AAL52897.1	1.62	5	11	328	Q-TOF
	BMEI1930	Leucine-, isoleucine-, valine-, threonine-, and alanine-binding protein precursor	AAL53111.1	1.61	2	7	133	Q-TOF
	BMEII0098	High affiny branched chain amino acid transport ATP-binding protein livF	AAL53339.1	1.38	3	10	166	Q-TOF
	BMEII0590	Sugar binding protein	AAL53832.1	2.68	11	27	781	Q-TOF
	BMEII0601	Cystine binding periplasmic protein	AAL53843.1	1.38	4	13	303	Q-TOF
	BMEII0734	Periplasmic oligopeptide Binding protein precursor	AAL53976.1	1.76	8	16	589	Q-TOF
	BMEII0923	Spermidine/putrescine-binding protein	AAL54165.1	1.52	3	9	193	Q-TOF
Unassigned	BMEI1201	Hypothetical cytosolic protein	AAL52382.1	2.64	6	17	477	Q-TOF
	BMEI1211	General L-amino acid-binding periplasmic protein AAPJ precursor	AAL52392.1	2.07	2	5	151	Q-TOF
	BMEI1747	aldehyde dehydrogenase	AAL52928.1	0.66	5	9	360	Q-TOF
	BMEI1819	Alcohol dehydrogenase deshydrogenase	AAL53000.1	1.44	3	7	192	Q-TOF
		Δ*vjbR*, pH 4−7						
A.A. metabolism	BMEI0101	Cysteine synthase A	AAL51283.1	0.68	2	7	147	Q-TOF
	BMEI0386	Succinate semialdehyde dehydrogenase	AAL51567.1	1.72	5	11	352	Q-TOF
	BMEI1925	Acetyl-CoA Carboxylase Alpha Chain/Propionyl-CoA Carboxylase Alpha Chain	AAL53106.1	0.75	4	5	244	Q-TOF
Central metabolism	BMEI0851	Enolase	AAL52032.1	0.56	5	11	311	Q-TOF
Nucleotide metabolism	BMEI0522	Carbamoyl Phosphate synthase large subunit	AAL51703.1	0.60	12	9	725	Q-TOF
	BMEI1127	Phosphoribosylformylglycinamidine Synthase	AAL52308.1	0.83	7	8	429	Q-TOF
Protein synthesis	BMEI0837	Glutamyl tRNA synthase	AAL52018.1	1.64	2	3	121	Q-TOF
	BMEI1047	Tyrosyl tRNA synthase	AAL52228.1	0.68	5	10	332	Q-TOF
Regulation	BMEI0417	PdhS	AAL51598.1	0.70	4	5	232	Q-TOF
	BMEI0558	Transcriptional regulator ArsR	AAL51739.1	0.68	5	15	389	Q-TOF
Replication/transcription	BMEI0880	Single strand binding protein	AAL52061.1	2.03	4	22	263	Q-TOF
Transport/secretion	BMEII0105	Iron regulated outer membrane protein FrpB	AAL53346.1	0.80	4	6	244	Q-TOF
		Δ*babR*, pH 7−11 NL						
Cell wall/envelope	BMEI1404	Mannosyltransferase	AAL52585.1	1.38	1119	35	151	Maldi-TOF
Other metabolism	BMEI0859	Lipoyl synthetase	AAL52040.1	0.52	14148	46	123	Maldi-TOF
		Δ*vjbR*, pH 7−11 NL						
A.a. metabolism	BMEI1970	*S*-adenosylmethionine synthetase	AAL53151.1	1.7	4	8	268	Q-TOF
Cell wall/envelope	BMEI0035	D-alanyl-D-alanine carboxypeptidase	AAL51217.1	1.42	25158	75	214	Maldi-TOF

Table 1. Continued

cellular function	BMEnnnnn	identification	accession no.	F.C.	# peptides	C %	score	method
	BMEI0575	UDP-*N*-acetylmuramoylalanyl-D-glutamyl-2,6-diaminopimelate-D-alanyl-D- alanyl ligase	AAL51756.1	3.26	11141	33	98	Maldi-TOF
	BMEI1029	Outer membrane protein TolC	AAL52210.1	4.22	16148	33	108	Maldi-TOF
	BMEI1435	Polysaccharide deacetylase	AAL52616.1	0.37	8115	45	103	Maldi-TOF
	BMEII0374	Alanine racemase	AAL53616.1	1.45	17121	50	110	Maldi-TOF
	BMEII1028	Tetraacyldisaccharide 4′-kinase	AAL54270.1	0.52	16127	62	147	Maldi-TOF
Protein synthesis	BMEI0741	23S rRNA methyltransferase	AAL51922.1	0.68	9144	55	73	Maldi-TOF
	BMEI0747	LSU ribosomal protein L10P	AAL51928.1	2.37	614	37	78	Maldi-TOF
	BMEI0753	SSU ribosomal protein S7P	AAL51934.1	1.93	5112	44	58	Maldi-TOF
	BMEI1169	SSU ribosomal protein S9P	AAL52350.1	1.93	317	17	42	Maldi-TOF
	BMEI1267	Dimethyladenosine transferase	AAL52448.1	0.40	1017	51	155	Maldi-TOF
Regulation	BMEI0808	Transcriptional Regulator, MerR Family	AAL51989.1	0.73	615	34	79	Maldi-TOF
Replication/transcription	BMEI1035	Atp-dependent rna helicase	AAL52216.1	1.5	4	9	268	Q-TOF
Transport/secretion	BMEI0469	Purine nucleoside permease	AAL51650.1	0.18	913	29	138	Maldi-TOF
	BMEII0032	Channel protein VirB8 homologue	AAL53273.1	0.26	912	53	157	Maldi-TOF
	BMEII0033	Channel protein VirB9 homologue	AAL53274.1	0.49	611	36	100	Maldi-TOF
	BMEII0593	Glucose ABC transporter ATPase	AAL53835.1	2.92	11116	45	133	Maldi-TOF
	BMEII0863	Oligopeptide transport ATP-binding protein appD	AAL54105.1	1.45	17124	38	183	Maldi-TOF
Unassigned	BMEI1193	Cell wall degradation protein	AAL52374.1	0.75	8117	18	69	Maldi-TOF
	BMEII0002	Ribosomal-protein-serine acetyltransferase	AAL53243.1	1.4	817	45	118	Maldi-TOF
	BMEII0431	Oxidoreductase	AAL53673.1	2.47	10115	26	109	Maldi-TOF

B

Gel	cellular function	BMEnnnnn	identification	accession no.	F.C.	sequence	C %	score	m/z	charge	method
Δ*babR*, pH 4−7											
	AA metabolism	BMEI0516	Aspartate aminotransferase	AAL51697.1	0.68	QAAIAAINR	2	51	464,2757	2+	Q-TOF
	Central metabolism	BMEI0791	Isocitrate deshydrogenase	AAL51972.1	0.68	ASFNYGLKR	2	49	528,2996	2+	Q-TOF
	Central metabolism	BMEI1436	pyruvate phosphate dikinase	AAL52617.1	0.47	TPQNITEEAR	1	68	579,815	2+	Q-TOF
	Stress/ chaperone	BMEI1367	Superoxide Dismutase Mn	AAL52548.1	1.38	LLEGSGLEGK	4	48	501,78	2+	Q-TOF
	Transport/ secretion	BMEII0593	ATP GDP Binding protein ABC transporter	AAL53835.1	1.93	SVFFDSASQTR	2	51	622,8208	2+	Q-TOF
	Unassigned	BMEI1939	D-3-phosphoglycerate dehydrogenase	AAL53120.1	0.60	GSLQNEPDILAALDR	4	121	806,4188	2+	Q-TOF
Δ*vjbR*, pH 7−11 NL											
	Cell wall/ envelope	BMEI0223	Membrane-bound lytic murein transglycosylase B	AAL51405.1	2.56	YAQATINADR	3	79	561,8065	2+	Q-TOF

[a] A. Proteins identified in the 2D-DIGE analysis of *babR* and *vjbR* mutant strains. B. Proteins identified by one single peptide in the 2D-DIGE analysis of *babR* and *vjbR* mutant strains. BMEnnnnn: ORF number; F.C.: fold change compared with the wild type strain; # peptides: numbers of unique peptides identified (for MALDI identification: number of peaks that match to the tryptic peptides vs. number of peaks that do not match to the tryptic peptides); C %: percentage sequence coverage of the protein; Score: identity score; Method: method used for the identification of the protein.

Impact of C_{12}−HSL on Selected QS Targets. To assess the effect of C_{12}−HSL on selected target genes, we performed qRT-PCR on total RNA extracted from *B. melitensis* 16 M and isogenic Δ*vjbR* and Δ*babR* mutants grown with or without C_{12}−HSL to an $OD_{600\ nm}$ of 0.7. Results are presented in Table 4; wt strain cultivated without addition of C_{12}−HSL was used as a benchmark. Regarding the expression of the genes encoding the two LuxR regulators in the parental strain, *vjbR* expression is repressed when exogenous C_{12}−HSL is added whereas *babR* expression is activated. The fact that the C_{12}−HSL effect on *vjbR* expression was observed in both the *B. melitensis* 16 M and the *babR* mutant suggests that VjbR regulates its own negative feedback loop. A similar proposal could be also suggested for BabR, but with a positive feedback loop.

Table 2. Targets Identified in This Study[a]

A

Gene/Protein	Subclasses	Identity/similarity/function	Ratio Δ*vjbR*/wt 2D-DIGE	Ratio Δ*babR*/wt 2D-DIGE	Ratio Δ*vjbR*/wt Microarra	Ratio Δ*babR*/wt Microarray	Ratio Δ*vjbR*/wt qRT-PCR	Ratio Δ*babR*/wt qRT-PCR	VirB Box	Operon	VjbR ChIP validation	Other Biological validation	Identified by Lamontagne et al.
BMEI0035	Cell wall/envelope	D-Alanyl-D-Alanine Carboxypeptidase	1,42	ND	1,10	1,01							
BMEI0223	Cell wall/envelope	Membrane Bound Lytic Murein Transglycolase	2,56	ND	1,62	1,15							
BMEI0575	Cell wall/envelope	UDP-N-Acetylmuramoylalanyl-D-Glutamyl-2,6-Diaminopimelate--D-Alanyl-D- Alanyl Ligase	3,26	ND	0,86	0,84							
BMEI0727	Cell wall/envelope	D-Alanine--D-Alanine Ligase A	ND	1,71	0,60	1,28							
BMEI1007	Cell wall/envelope	25 kDa Outer-Membrane Immunogenic Protein Precursor	ND	ND	6,52	0,83			+		+	VjbR	
BMEI1029	Cell wall/envelope	Outer Membrane Protein TolC	4,22	ND	1,30	1,05							
BMEI1305	Cell wall/envelope	Porin	ND	ND	5,70	0,88					+	VjbR	+
BMEI1404	Cell wall/envelope	Mannosyltransferase	ND	1,38	1,09	0,92							
BMEI1435	Cell wall/envelope	Polysaccharide Deacetylase	0,37	ND	0,77	1,22							
BMEII0017	Cell wall/envelope	Omp10	ND	ND	1,47	1,09						VjbR	
BMEII0374	Cell wall/envelope	Alanine Racemase	1,41	ND	0,97	1,01							
BMEII0844	Cell wall/envelope	31 kDa Outer-Membrane Immunogenic Protein Precursor	ND	ND	2,21	1,09						VjbR	
BMEII1028	Cell wall/envelope	Tetraacyldisaccharide 4'-Kinase	0,52	ND	0,88	0,95							
BMEI0258	Transport/secretion	High-Affinity Branched-Chain Amino Acid Transport System Permease Protein LivH	ND	ND	1,50	0,98	2,14	ND					
BMEI0469	Transport/secretion	Purine Nucleoside Permease	0,18	ND	0,45	1,35							
BMEI1716	Transport/secretion	Trehalose/Maltose Binding Protein	ND	1,62	1,70	1,11							+
BMEI1930	Transport/secretion	Leucine-, Isoleucine-, Valine-, Threonine-, and Alanine-Binding Protein Precursor	ND	1,61	1,45	0,91							
BMEII0025	Transport/secretion	Attachment Mediating Protein VirB1 Homolog	ND	ND	0,15	1,43	0,04	1,92	+	+	+	VjbR	
BMEII0026	Transport/secretion	Attachment Mediating Protein VirB2 Homolog	ND	ND	0,11	1,57	0,05	2,14	+	+	+	VjbR	
BMEII0027	Transport/secretion	Channel Protein VirB3 Homolog	ND	ND	0,15	1,56				+		VjbR	
BMEII0028	Transport/secretion	ATPase VirB4 Homolog	ND	ND	0,33	1,56				+		VjbR	
BMEII0029	Transport/secretion	Attachment Mediating Protein VirB5 Homolog	ND	ND	0,26	1,37				+		VjbR	
BMEII0030	Transport/secretion	Channel Protein VirB6 Homolog	ND	ND	0,61	1,26				+		VjbR	
BMEII0032	Transport/secretion	Channel Protein VirB8 Homolog	0,26	ND	0,50	1,55				+		VjbR	
BMEII0033	Transport/secretion	Channel Protein VirB9 Homolog	0,49	ND	0,72	1,58				+		VjbR	
BMEII0105	Transport/secretion	iron regulated outer membrane protein FrpB	0,80	ND	1,06	1,15							
BMEII0098	Transport/secretion	High Affiny Branched Chain Amino Acid Transport ATP-Binding Protein LivF	ND	1,38	0,84	0,93							
BMEII0340	Transport/secretion	High-Affinity Branched-Chain Amino Acid Transport System Permease Protein LivM	ND	ND	2,68	1,09				+			
BMEII0341	Transport/secretion	High-Affinity Branched-Chain Amino Acid Transport System Permease Protein LivH	ND	ND	2,33	1,03				+			
BMEII0342	Transport/secretion	High-Affinity Branched-Chain Amino Acid Transport ATP-Binding Protein LivF	ND	ND	2,39	0,85				+			
BMEII0343	Transport/secretion	High-Affinity Branched-Chain Amino Acid Transport ATP-Binding Protein LivG	ND	ND	2,00	0,96				+			
BMEII0590	Transport/secretion	Sugar-Binding Protein	ND	2,68	6,56	0,77					+		+
BMEII0591	Transport/secretion	Sugar Transport System Permease Protein	ND	ND	4,62	0,93				+			
BMEII0592	Transport/secretion	Sugar Transport System Permease Protein	ND	ND	3,49	0,87				+			
BMEII0593	Transport/secretion	Glucose ABC Transporter ATPase	2,92	1,93	1,62	1,05				+			
BMEII0601	Transport/secretion	Cysteine Binding Periplasmic Protein	ND	1,38	1,12	1,01							
BMEII0625	Transport/secretion	Glycerol-3-Phosphate-Binding Periplasmic Protein Precursor	ND	ND	5,58	0,82	1,49	ND					
BMEII0734	Transport/secretion	Periplasmic Oligopeptide-Binding Protein Precursor	ND	1,76	15,92	1,09				+	+		+
BMEII0735	Transport/secretion	Periplasmic Oligopeptide-Binding Protein Precursor	ND	ND	5,82	1,05				+			+
BMEII0736	Transport/secretion	Oligopeptide Transport System Permease Protein OppB	ND	ND	3,72	1,04				+			
BMEII0737	Transport/secretion	Oligopeptide Transport System Permease Protein OppC	ND	ND	5,01	1,11				+			
BMEII0738	Transport/secretion	Oligopeptide Transport ATP-Binding Protein OppD	ND	ND	2,32	1,03				+			+
BMEII0863	Transport/secretion	Oligopeptide Transport ATP-Binding Protein AppD	1,45	ND	0,88	1,08							
BMEII0923	Transport/secretion	Spermidine/Putrescine-Binding Protein	ND	1,52	1,99	0,77							

B

Gene/Protein	Subclasses	Identity/similarity/function	Ratio Δ*vjbR*/wt 2D-DIGE	Ratio Δ*babR*/wt 2D-DIGE	Ratio Δ*vjbR*/wt Microarra y	Ratio Δ*babR*/wt Microarray	Ratio Δ*vjbR*/wt qRT-PCR	Ratio Δ*babR*/wt qRT-PCR	VirB Box	Operon	VjbR ChIP validation	Other Biological validation	Identified by Lamontagne et al.
BMEI0101	AA Metabolism	Cysteine Synthase A	0,68	ND	1,05	1,37							
BMEI0231	AA Metabolism	NAD Specific Glutamate Dehydrogenase	ND	0,37	1,41	1,11							+
BMEI0386	AA Metabolism	Succinate Semialdehyde Dehydrogenase	1,72	ND	1,40	1,09	2,33	ND					
BMEI0451	AA Metabolism	2-Isopropyl Malate Synthase	ND	0,21	0,95	1,11							
BMEI0516	AA Metabolism	Aspartate Aminotransferase A	ND	0,68	1,47	1,20							
BMEI0811	AA Metabolism	L-Serine Dehydratase	ND	0,66	0,78	1,02							
BMEI0979	AA Metabolism	Glutamine Synthase	ND	0,30	1,18	1,26							
BMEI1620	AA Metabolism	Ornithine Carbamoyltransferase	ND	0,64	1,00	1,20							
BMEI1638	AA Metabolism	Glutamate Synthase (NADPH) Small Chain	ND	2,21	2,31	0,74							
BMEI1925	AA Metabolism	Acetyl-CoA Carboxylase Alpha Chain / Propionyl-CoA Carboxylase Alpha Chain	0,75	ND	1,84	1,14							
BMEI1970	AA Metabolism	S Adenosylmethionine Synthetase	1,70	ND	1,57	1,21							
BMEII0371	AA Metabolism	β-alanine pyruvate transaminase	ND	1,78	1,97	0,97							
BMEII0559	AA Metabolism	Aminomethyltransferase	ND	1,68	1,03	1,03							
BMEI0310	Carbohydrate metabolism	Glyceraldehyde 3-Phosphate Deshydrogenase	ND	1,44	1,49	1,12							
BMEI1413	Carbohydrate metabolism	GDP-Mannose 4,6-Dehydratase	ND	0,68	1,56	1,23							+
BMEI1779	Carbohydrate metabolism	Fructokinase	ND	1,61	1,05	0,97							
BMEII0358	Carbohydrate metabolism	2-Dehydro-3-Deoxyphosphogalactonate Aldolase	ND	1,38	0,93	0,94							
BMEII0511	Carbohydrate metabolism	Phosphogluconate Dehydratase	ND	0,08	0,91	0,95							
BMEI0138	Central metabolism	Succinyl CoA Synthetase Beta Chain	ND	1,91	1,09	0,77							
BMEI0161	Central metabolism	Succinate Dehydrogenase	ND	0,16	1,29	1,13				+			+
BMEI0791	Central metabolism	Isocitrate Dehydrogenase (NADP)	ND	0,68	1,54	1,05	1,47	ND					
BMEI0836	Central metabolism	Citrate Synthase	ND	0,56	1,63	1,09	1,94	ND					
BMEI0851	Central metabolism	Enolase	1,34	0,56	1,62	0,92	1,60	ND					+
BMEI1436	Central metabolism	Pyruvate Phosphate Dikinase	ND	0,47	1,05	1,10							
BMEII0248	Central metabolism	Phosphoglycerate Mutase	ND	1,74	1,22	1,05							
BMEII0423	Central metabolism	Fructose-Bisphosphate Aldolase	ND	ND	1,54	0,89	3,62	ND					
BMEI0543	Lipid metabolism	Cholоylglycine Hydrolase	ND	0,11	1,58	0,95	1,52	ND				VjbR/BabR	
BMEI1112	Lipid metabolism	3-Oxo-Acyl-Carrier Protein Synthase	ND	1,65	0,89	0,93							
BMEI1196	Lipid metabolism	EnoylCoA Hydratase	ND	1,51	1,08	1,00							
BMEI1512	Lipid metabolism	Enoyl-(acyl carrier protein) reductase	ND	0,74	1,84	1,08							
BMEI0522	Nucleotide metabolism	Carbamoyl Phosphate Synthase Large Subunit	0,60	ND	1,11	1,04							
BMEI1127	Nucleotide metabolism	Phosphoribosylformylglycinamidine Synthase	0,83	ND	0,95	1,07							
BMEI1643	Nucleotide metabolism	N Carbamoyl L Amino Acid Amidohydrolase	ND	1,62	1,26	0,77							
BMEI0176	Other metabolism	Porphobilinogene Deaminase	ND	0,13	1,11	1,03							
BMEI0219	Other metabolism	Malonate-Semialdehyde Dehydrogenase (Acylating) / Methylmalonate-Semialdehyde Dehydrogenase (Acylating)	ND	0,51	3,27	0,67							
BMEI0222	Other metabolism	Carbonic Anhydrase	ND	ND	1,74	1,22			+			VjbR	
BMEI0712	Other metabolism	CbiG Protein / Precorrin-3B C17-Methyltransferase	ND	0,08	0,98	1,07							
BMEI0859	Other metabolism	Lipoyl Synthetase	ND	1,23	1,30	1,23							
BMEI1588	Other metabolism	Carboxynorspermidine dehydrogenase	ND	0,72	1,06	1,11							

Table 2. Continued

C

Gene/Protein	Subclasses	Identity/similarity/function	Ratio ΔvjbR/wt 2D-DIGE	Ratio ΔbabR/wt 2D-DIGE	Ratio ΔvjbR/wt Microarray	Ratio ΔbabR/wt Microarray	Ratio ΔvjbR/wt qRT-PCR	Ratio ΔbabR/wt qRT-PCR	VirB Box	Operon	VjbR ChIP validation	Other Biological validation	Identified by Lamontagne et al.
BMEI0056	Protein synthesis	LSU Ribosomal Protein L28P	ND	ND	2,27	1,34	2,44	1,30					
BMEI0481	Protein synthesis	LSU Ribosomal Protein L25P	ND	0,71	1,58	1,16							
BMEI0741	Protein synthesis	23S rRNA methyltransferase	0,68	ND	1,03	1,01							
BMEI0742	Protein synthesis	Protein Translation Elongation Factor Tu (EF-Tu)	ND	1,98	1,81	1,30							+
BMEI0747	Protein synthesis	LSU Ribosomal Protein L10P	2,37	ND	1,38	1,22							
BMEI0753	Protein synthesis	SSU Ribosomal Protein S7P	1,93	ND	1,37	1,26				+			+
BMEI0754	Protein synthesis	Protein Translation Elongation Factor G (EF-G)	ND	ND	1,71	1,28				+			+
BMEI0837	Protein synthesis	Glutamyl Trna Synthase	1,64	ND	0,99	0,91							
BMEI1047	Protein synthesis	Tyrosyl tRNA Synthase	0,68	ND	1,23	1,07							
BMEI1169	Protein synthesis	SSU Ribosomal Protein S9P	1,93	ND	1,26	0,99				+			
BMEI1267	Protein synthesis	Dimethyladenosine Transferase	0,40	ND	1,03	1,06							
BMEI1480	Protein synthesis	SSU Ribosomal Protein S6P	ND	ND	2,09	1,35	1,56	ND		+			
BMEI1481	Protein synthesis	SSU Ribosomal Protein S18P	ND	ND	1,76	1,27				+			
BMEI1483	Protein synthesis	LSU Ribosomal Protein L9P	ND	0,12	1,45	1,15							
BMEI1915	Protein synthesis	SSU Ribosomal Protein S1P	ND	1,77	1,26	1,46							+

D

Gene/Protein	Subclasses	Identity/similarity/function	Ratio ΔvjbR/wt 2D-DIGE	Ratio ΔbabR/wt 2D-DIGE	Ratio ΔvjbR/wt Microarray	Ratio ΔbabR/wt Microarray	Ratio ΔvjbR/wt qRT-PCR	Ratio ΔbabR/wt qRT-PCR	VirB Box	Operon	VjbR ChIP validation	Other Biological validation	Identified by Lamontagne et al.
BMEI0096	Respiration	Electron Transfer Flavoprotein Beta Subunit	ND	1,54	1,00	0,89							
BMEI0248	Respiration	ATP Synthase Delta Chain	ND	ND	1,47	1,08				+			
BMEI0249	Respiration	ATP Synthase Alpha Chain	ND	0,76	2,09	1,25				+			+
BMEI0473	Respiration	Ubiquinol-Cytochrome C Reductase Iron-Sulfur Subunit	ND	ND	2,10	0,97				+			
BMEI0474	Respiration	Cytochrome B	ND	ND	2,26	0,97	1,55	ND		+			+
BMEI0487	Respiration	ATP Synthase Beta Subunit/Transription Termination Factor Rho	ND	1,61	0,96	1,01							
BMEI1465	Respiration	Cytochrome C Oxidase Polypeptide I	ND	ND	2,01	1,09	1,59	ND		+			
BMEI1466	Respiration	Cytochrome C Oxidase Polypeptide I	ND	ND	1,51	1,05			+	+			
BMEI1564	Respiration	Cytochrome C Oxidase Polypeptide I Homolog, Bacteroid	ND	ND	2,09	0,90	15,67	ND		+			
BMEI1565	Respiration	Cytochrome C Oxidase, Monoheme Subunit, Membrane-Bound	ND	ND	1,65	0,98			+	+			
BMEI1898	Respiration	Cytochrome O Ubiquinol Oxidase Operon Protein CyoD	ND	ND	0,52	1,06	0,70	ND	+	+			
BMEI1899	Respiration	Cytochrome O Ubiquinol Oxidase Subunit III	ND	ND	0,48	1,00			+	+			
BMEI1900	Respiration	Cytochrome O Ubiquinol Oxidase Subunit I	ND	ND	0,45	1,18			+	+			

E

Gene/Protein	Subclasses	Identity/similarity/function	Ratio ΔvjbR/wt 2D-DIGE	Ratio ΔbabR/wt 2D-DIGE	Ratio ΔvjbR/wt Microarray	Ratio ΔbabR/wt Microarray	Ratio ΔvjbR/wt qRT-PCR	Ratio ΔbabR/wt qRT-PCR	VirB Box	operon	VjbR ChIP validation	Other Biological validation	Identified by Lamontagne et al.
BMEI0123	Stress/chaperone	Peptidyl-Prolyl Cis-Trans Isomerase	ND	1,52	1,06	0,97							
BMEI0195	Stress/chaperone	ATP-Dependent Clp Protease, ATP-Binding Subunit ClpB	ND	0,74	1,26	1,57							
BMEI0613	Stress/chaperone	Protease DO	ND	1,66	0,73	1,01							
BMEI0816	Stress/chaperone	ATP-Dependent Clp Protease ATP-Binding Subunit ClpA	ND	ND	0,88	1,35	ND	1,29					
BMEI0874	Stress/chaperone	ATP-Dependent Clp Protease Proteolytic Subunit	ND	ND	1,66	1,49	1,39	ND					
BMEI1129	Stress/chaperone	Glutaredoxin	ND	ND	1,35	1,04	1,49	ND					
BMEI1367	Stress/chaperone	Superoxide Dismutase Mn	ND	1,38	1,79	1,12							
BMEI2002	Stress/chaperone	DnaK Protein	ND	1,78	1,10	1,63	ND	1,30					+
BMEI2022	Stress/chaperone	Thioredoxin C-1	ND	ND	2,18	0,94	1,40	ND					+
BMEII0401	Stress/chaperone	Thioredoxine	ND	1,71	0,96	1,00							
BMEII0581	Stress/chaperone	Superoxide Dismutase (Cu-Zn) SodC	ND	ND	1,74	1,17	1,82	ND					+
BMEII0891	Stress/chaperone	Disulfide Bond Formation Protein B	ND	ND	1,45	1,16	1,27	ND					
BMEII1047	Stress/chaperone	10 kDa Chaperonin GroES	ND	ND	0,49	2,95	0,42	3,19					
BMEII1048	Stress/chaperone	60 kDa Chaperonin GroEL	ND	0,63	0,35	3,19	0,39	4,51					+

F

Gene/Protein	Subclasses	Identity/similarity/function	Ratio ΔvjbR/wt 2D-DIGE	Ratio ΔbabR/wt 2D-DIGE	Ratio ΔvjbR/wt Microarray	Ratio ΔbabR/wt Microarray	Ratio ΔvjbR/wt qRT-PCR	Ratio ΔbabR/wt qRT-PCR	VirB Box	operon	VjbR ChIP validation	Other Biological validation	Identified by Lamontagne et al.
BMEI0417	Regulation	PdhS	0,70	ND	0,91	1,20							
BMEI0558	Regulation	Transcriptional Regulator ArsR	0,68	ND	1,05	1,13							
BMEI0626	Regulation	Transcriptional Regulator, GntR Family	ND	2,64	3,42	1,13							+
BMEI0808	Regulation	Transcriptional Regulator, MerR Family	0,73	ND	0,73	0,84							
BMEI0872	Regulation	Hfq	ND	ND	1,76	1,00	1,63	ND					
BMEI1758	Regulation	Transcriptional Activator, LuxR Family (BabR)	ND	ND	0,51	-	0,68	-					
BMEII0299	Regulation	IclR family transcriptional regulator	ND	0,73	0,87	0,96							
BMEII1116	Regulation	Transcriptional Activator, LuxR Family (VjbR)	ND	0,55	-	1,44	-	1,29					
BMEI0588	Replication/transcription	DNA Repair Protein RecN	ND	0,21	1,00	0,99							
BMEI0749	Replication/transcription	DNA-Directed RNA Polymerase Beta Chain	ND	0,30	1,10	1,20							+
BMEI0880	Replication/transcription	Single Strand Binding Protein	2,03	ND	1,02	1,11							
BMEI1035	Replication/transcription	ATP-dependent RNA helicase	1,50	ND	1,30	1,13							
BMEI1823	Replication/transcription	DNA Gyrase B	ND	0,60	0,80	1,20							

G

Gene/Protein	Subclasses	Identity/similarity/function	Ratio ΔvjbR/wt 2D-DIGE	Ratio ΔbabR/wt 2D-DIGE	Ratio ΔvjbR/wt Microarray	Ratio ΔbabR/wt Microarray	Ratio ΔvjbR/wt qRT-PCR	Ratio ΔbabR/wt qRT-PCR	VirB Box	operon	VjbR ChIP validation	Other Biological validation	Identified by Lamontagne et al.
BMEI0030	-	Hypothetical Cytosolic Protein	ND	ND	0,25	1,10					+		
BMEI0587	-	ComL, Competence Lipoprotein	ND	ND	1,62	1,06			+	+			
BMEI0668	-	Calcium Binding Protein	ND	ND	5,77	0,59	2,61	0,37			+		
BMEI1193	-	Cell wall degradation protein	0,75	ND	1,38	1,12							
BMEI1201	-	Hypothetical Cytosolic Protein	ND	2,64	1,08	1,05							
BMEI1211	-	General L-Amino Acid-Binding Periplasmic Protein AapJ Precursor	ND	2,07	2,05	0,80							
BMEI1747	-	Aldehyde Dehydrogenase	ND	0,66	2,37	1,97							
BMEI1819	-	Alcohol Dehydrogenase	ND	1,44	1,35	1,05							+
BMEI1939	-	D-3-Phosphoglycerate Dehydrogenase	ND	0,60	0,81	0,97							
BMEII0002	-	Ribosomal-Protein-Serine Acetyltransferase	1,40	ND	1,17	1,04							
BMEII0431	-	Oxidoreductase	1,40	ND	0,89	0,87							

[a] Summary table of targets genes identified in this study and connections with other published results. Each target is defined by a BMEnnnnn number (corresponding to the ORF number of the gene in *Brucella melitensis* 16 M genome), a functional class and a predicted function. A: Cell wall biogenesis and transport/secretion subclasses. B: Metabolism subclass. C: Translation subclass. D: Respiration process subclass. E: Stress response subclass. F: Regulation subclass. G: Unclassified targets. In the fold change column, colors represent the regulator's effect: red when the regulator exerts a repressive role (fold change >1.3) and green when the regulator exerts an activation role (fold change <0.7). Light colors were used for genes with a lower fold change (pink: 1.3 > fold change >1.2; olive-green: 0.8 > fold change >0.7). Twenty-nine targets of interest were analyzed by qRT-PCR on new biological samples to validate microarray results. These results are listed in the "Ratio mutant/wt qRT-PCR" column. The "VirB Box" column indicates with a "+" genes containing in their promoter sequence the box identified by de Jong[35] for VjbR regulation. "Operon" column indicates genes which are predicted by BioCyc or KEGG DAS to be part of an operon. Positive results for VjbR ChIP experiments are labeled with a "+" in the "VjbR ChIP validation" column. When biological validations were available (such as Western blots, bile salts resistance test.. .), mutant strain's name tested can been found in the "Biological validation" column. In the last column, genes identified by a "+" have been found by Lamontagne and coworkers[17] to be implicated in *Brucella abortus* intracellular adaptation. ND: not determined.

Table 3. VjbR and BabR Shared Targets: ORFs Identified by the Proteomic and Transcriptomic Analyses and Regulated by Both LuxR Type Regulators

	target	identity/similarity/function	ratio Δ*vjbR*/wt	ratio Δ*babR*/wt
Co-regulated targets	BMEI0056	LSU Ribosomal Protein L28P	2.27	1.34
	BMEI0195	ATP-Dependent Clp Protease, ATP-Binding Subunit ClpB	1.26	1.57
	BMEI0223	Membrane Bound Lytic Murein Transglycolase	2.56	1.38
	BMEI0742	Protein Translation Elongation Factor Tu (EF-Tu)	1.81	1.30
	BMEI0753	SSU Ribosomal Protein S7P	1.37	1.26
	BMEI0754	Protein Translation Elongation Factor G (EF-G)	1.71	1.28
	BMEI0874	ATP-Dependent Clp Protease Proteolytic Subunit	1.66	1.49
	BMEI1480	SSU Ribosomal Protein S6P	2.09	1.35
	BMEI1481	SSU Ribosomal Protein S18P	1.76	1.27
	BMEI1747	Aldehyde Dehydrogenase	2.37	1.98
	BMEI1915	SSU Ribosomal Protein S1P	1.26	1.46
	BMEII0593	Glucose ABC Transporter ATPase	2.92	1.93
Differentially regulated targets	BMEI0219	Malonate-Semialdehyde Dehydrogenase (Acylating)/ Methylmalonate-Semialdehyde Dehydrogenase (Acylating)	3.27	0.67
	BMEI0469	Purine Nucleoside Permease	0.45	1.35
	BMEI0668	Calcium Binding Protein	5.77	0.59
	BMEI0727	D-Alanine-D-Alanine Ligase A	0.60	1.28
	BMEI0851	Enolase	0.56	1.34
	BMEII0025	Attachment Mediating Protein VirB1 Homologue	0.15	1.43
	BMEII0026	Attachment Mediating Protein VirB2 Homologue	0.11	1.57
	BMEII0027	Channel Protein VirB3 Homologue	0.15	1.56
	BMEII0028	ATPase VirB4 Homologue	0.33	1.56
	BMEII0029	Attachment Mediating Protein VirB5 Homologue	0.26	1.37
	BMEII0030	Channel Protein VirB6 Homologue	0.61	1.26
	BMEII0032	Channel Protein VirB8 Homologue	0.50	1.55
	BMEII0033	Channel Protein VirB9 Homologue	0.72	1.58
	BMEII1047	10 kDa Chaperonin GroES	0.49	2.95
	BMEII1048	60 kDa Chaperonin GroEL	0.35	3.19

Table 4. Validation of Some Targets by qRT-PCR and Analysis of C_{12}−HSL Effect[a]

	babR	*vjbR*	*dnaK*	*virB2*	*groEL*	*groES*	BMEI0433	BMEI0668	BMEII0625
wt + ACN	1.0	1.0	1.0	1.0	1.0	1.0	1.0	1.0	1.0
wt + C_{12}−HSL	2.6	0.5	1.6	0.2	2.0	2.2	2.1	4.5	1.8
Δ*babR* + ACN	0	1.7	1.9	1.9	3.1	2.7	1.1	0.6	0.8
Δ*babR* + C_{12}−HSL	0	0.3	1.8	0.1	4.0	3.3	0.8	3.5	2.2
Δ*vjbR* + ACN	0.7	0	0.9	0.1	0.1	0.1	2.9	4.5	3.8
Δ*vjbR* + C_{12}−HSL	1.5	0	1.2	0.1	0.2	0.2	4.4	9.7	4.9

[a] Comparison of fold change ratios for mRNA from wt, Δ*babR* and Δ*vjbR* strains with or without C_{12}−HSL. RNA was extracted at an equivalent OD600 for the transcriptomic and the qRT-PCR experiments. ACN: Acetonitrile: C_{12}−HSL solvent. C_{12}−HSL: dodecanoyl-L-homoserine lactone (added to the culture media at a final concentration of 5 mM). We considered that gene expression is different between wt and mutant strain when the ratio is >1.3 or <0.7.

Table 4 shows that, except for *virB*2 and *vjb*R, C_{12}−HSL activates the expression of target genes in *B. melitensis* 16 M. Interestingly, depending on the target gene, the C_{12}−HSL activating effect seems to be mostly dependent either on BabR (e.g., BMEI0433), VjbR (*e.g. dnaK*) or both regulators (e.g., BMEI0668 and BMEII0625). Because the effect of C_{12}−HSL on some targets (e.g., BMEI0433) is still observed in the Δ*vjbR* strain (but not in the Δ*babR* strain) and VjbR and BabR are the only predicted proteins possessing a predicted AHL-binding domain in *B. melitensis* 16 M, this result is the first evidence suggesting that BabR can respond to C_{12}−HSL. The fact that two regulators react to the same signal molecule is quite unusual. One possibility could be that the two regulators have a different affinity for the C_{12}−HSL. For example VjbR may respond to a lower level of AHLs once inside the cell and when a higher AHL concentration is reached, BabR may be activated. This will be an interesting hypothesis to test since we propose that BabR can modulate VjbR activity. Nevertheless, we cannot exclude the possibility that other unidentified AHLs may act preferentially on one or the other LuxR-type regulator.

Global Impact of QS on *Brucella melitensis* 16 M. Cell Wall/Envelope Biogenesis and Transport/Secretion Proteins. As shown in Table 2A, VjbR and BabR affect many genes involved in cell envelope biogenesis and membrane transport. These genes constitute the largest class identified in the *B. melitensis* 16 M QS regulon. As expected from previous work in our laboratory,[19,28] the involvement of VjbR in the regulation of genes encoding components of the type four secretion system (T4SS) and outer membrane proteins (OMP) is observed. The identification of numerous membrane proteins whose genes are regulated by VjbR in this analysis further emphasized the role of VjbR in the control of membrane components. Interestingly, in addition to genes encoding OMPs, several genes predicted to be involved in murein and polysaccharide synthesis and LPS biogenesis are also regulated by VjbR.

Regarding the T4SS, a major component in *Brucella* virulence, we note a clear and inverse regulatory effect between the two LuxR regulators. VjbR activates the transcription of the *vir*B operon (as previously described[19,28]), while BabR had a

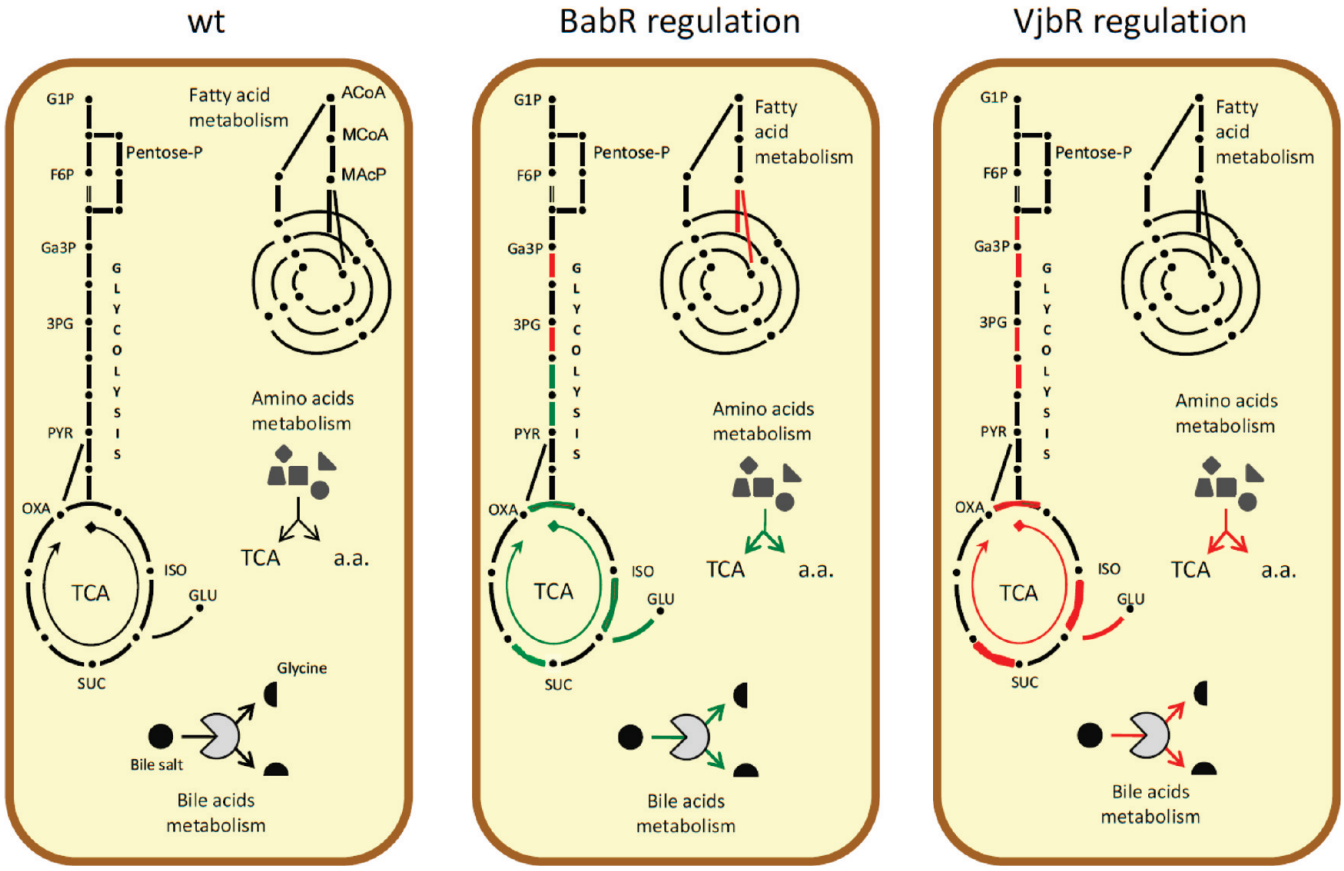

Figure 1. Diagram representing the main metabolic pathways in the wt strain and the regulation effect of VjbR and BabR. Pentose-P, pentose phosphate pathway; TCA, tricarboxylic acid cycle; G1P, glycerol-1-P; F6P, fructose-6-P; Ga3P, glyceraldehyde-3-P; 3PG, 3-P-glycerate; PYR, pyruvate; OXA, oxaloacetate; ISO, isocitrate; SUC; succinate; GLU, glutamate; Bile salt, glycocholate or taurocholate. Red lines/arrows represent repressed pathways while green lines/arrows represent activated pathways by the regulator. a.a., amino acid.

repressing effect on these genes. This observation was confirmed by two independent qRT-PCR experiments (Tables 2 and 4).

Numerous genes predicted to be involved in amino acid, oligopeptide and sugar transport were found to be QS targets in *B. melitensis* 16 M (Table 2A) and many of these genes appear to be regulated by VjbR. The fact that a lot of genes putatively involved in amino acid and sugar transport are part of the QS regulon suggests that a metabolic switch could be initiated by QS.

Metabolism Pathways. As can be seen in Table 2B, our analyses of *vjbR* and *babR* mutants revealed that numerous genes and/or proteins involved in metabolic pathways are regulated by QS in the parental 16 M strain. Figure 1 presents a schematic view of the main central metabolic pathways in *B. melitensis* 16 M, and the effects of *vjbR* and *babR* mutations on these pathways. Transcriptomic analysis revealed that VjbR exerts a repressive effect on numerous genes encoding enzymes involved in TCA cycle and glycolysis. As for BabR, proteomic analysis showed an activation effect on these two pathways. Interestingly, this same group of targets, constituted by BMEI0851 (enolase), BMEI0836 (citrate synthase), BMEI0791 (isocitrate dehydrogenase), BMEI0161 and BMEI0162 (succinate dehydrogenases) and BMEI0231 (NAD specific glutamate dehydrogenase) was regulated differentially depending upon the LuxR regulator, suggesting that QS could have a global reorganization effect on central metabolic processes. BabR also exerts a repressive effect on fatty acid metabolism genes in the parental strain.

Both LuxR regulators also have a strong regulatory effect on BMEI0543 (a gene coding for a choloylglycine hydrolase). VjbR repressed the transcription of *cgh* (transcriptional fold change = 1.58) while BabR strongly activated the production of CGH (proteomic fold change = 0.11). A recent study in *B. abortus* has demonstrated the involvement of *cgh* in successful infection of mice through the oral route.[48] Interestingly CGH is found in *Brucella* culture supernatants and its secretion seems to be VirB-dependent as demonstrated by the analysis of *B. abortus* wt and *virB* mutant strains.[49] *Brucella* QS regulators could thus be involved not only in the regulation of the genes encoding the VirB machinery but also in the regulation of the genes encoding the effectors it secretes. Consequently, we tested the resistance of QS mutants to bile salts. As shown Figure 2, the Δ*babR* strain was significantly more sensitive to bile salts than the *B. melitensis*16 M. In contrast, the Δ*vjbR* strain displayed an enhanced resistance to bile salts, supplying a biological validation of our proteomic/transcriptomic analysis.

Despite the fact that VjbR and BabR regulate in an opposite way the same group of genes encoding central metabolic enzymes, we never observed a growth delay for the *vjbR* and *babR* mutant strains in liquid or solid culture in rich media (see for example Figure 1A). However, using the Biotype 100 system (Biomerieux), we noted some differences in carbon substrate assimilation between the parental strain and the *vjbR*

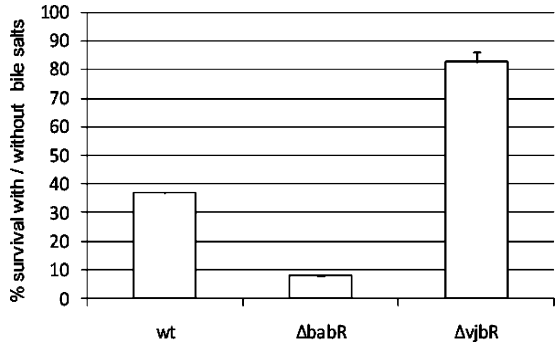

Figure 2. wt, Δ*vjbR* and Δ*babR* resistance to bile salts. Strains were growth in 2YT with bile salts and CFU were compared with cultures in 2YT (100% of survival). Error bars represent standard deviation from three independent experiments. CFU, colony forming unit.

and *babR* mutants (data not shown). So the role of the corresponding LuxR regulators in regulating metabolic pathways is worthy of further investigation.

Protein Synthesis and Respiration. Numerous genes coding for ribosomal proteins (LSU and SSU ribosomal proteins) and translation factors (EF-Tu, EF-G) are repressed by VjbR and to a lesser extent by BabR suggesting that these regulators depress protein synthesis (Table 2C). As can be seen in Table 2D, VjbR modulates the expression of genes encoding the terminal oxidases of the respiratory chain (activating the ubiquinol oxidase gene (*cyo*) and repressing the cytochrome C oxidase genes *coxA* (BMEI1465), *coxB* (BMEI1466) *ccoN* (BMEI1565) and *ccoO* (BMEI1564). BabR does not appear to control the expression of these cytochrome genes.

Stress Responses. Our study suggests that a fraction of the QS targets in *B. melitensis* 16 M may be involved in stress responses (Table 2E). VjbR targets belonging to this category are essentially involved in protein folding (*groES* and *groEL* are activated by VjbR and repressed by BabR) and thiol-disulfide exchange (BMEI1129 and BMEI2022 encoding respectively a glutaredoxin and a thioredoxin are repressed by VjbR). BabR repressed many genes belonging to this functional group. These include *clpP*, *clpA*, and genes coding for the chaperones GroES, GroEL and DnaK, a chaperone identified as necessary for *B. suis* survival in macrophages.[50] To further examine the role of QS in stress responses in *B. melitensis* 16 M, we tested the resistance of both Δ*vjbR* and Δ*babR* mutants to several kinds of stresses. The two QS mutants behave as the parental strain during the growth at pH 5, pH 7 (figure 3) and at pH 4, pH 6 and pH 8 (data not shown). In contrast, the *vjbR* mutant seems to be delayed its the adaptation to alkaline pH (pH 9). The response of *Brucella* strains to alkaline stress has not been described, but Appelbe et al. have shown that *dnaK* and *groEL* are induced during alkaline stress in *Enterococcus faecalis*.[51] While numerous genes encoding stress response proteins involved in adaptation to oxidative stress (*hfq*, *clpA*, *clpB*, *sodC*...) are regulated trough VjbR and BabR in *B. melitensis* 16 M, neither of the QS mutants displayed a higher sensitivity to H_2O_2 than the parent strain (data not shown). Likewise, the *vjbR* and Δ*babR* mutants were also insensitive to cold or heat shock (data not shown).

Regulation, DNA Replication and Transcription. In addition to the cross talk between the two QS regulators described above, other regulators are part of the QS regulon (Table 2F): PdhS, a histidine kinase involved in cell cycle control,[52] and four putative transcriptional regulators of the families ArsR, GntR, IclR and MerR.

VjbR represses the transcription of *hfq*, a RNA chaperone that binds small regulatory RNA (sRNAs) and mRNAs to facilitate translational regulation in response to envelope stress,

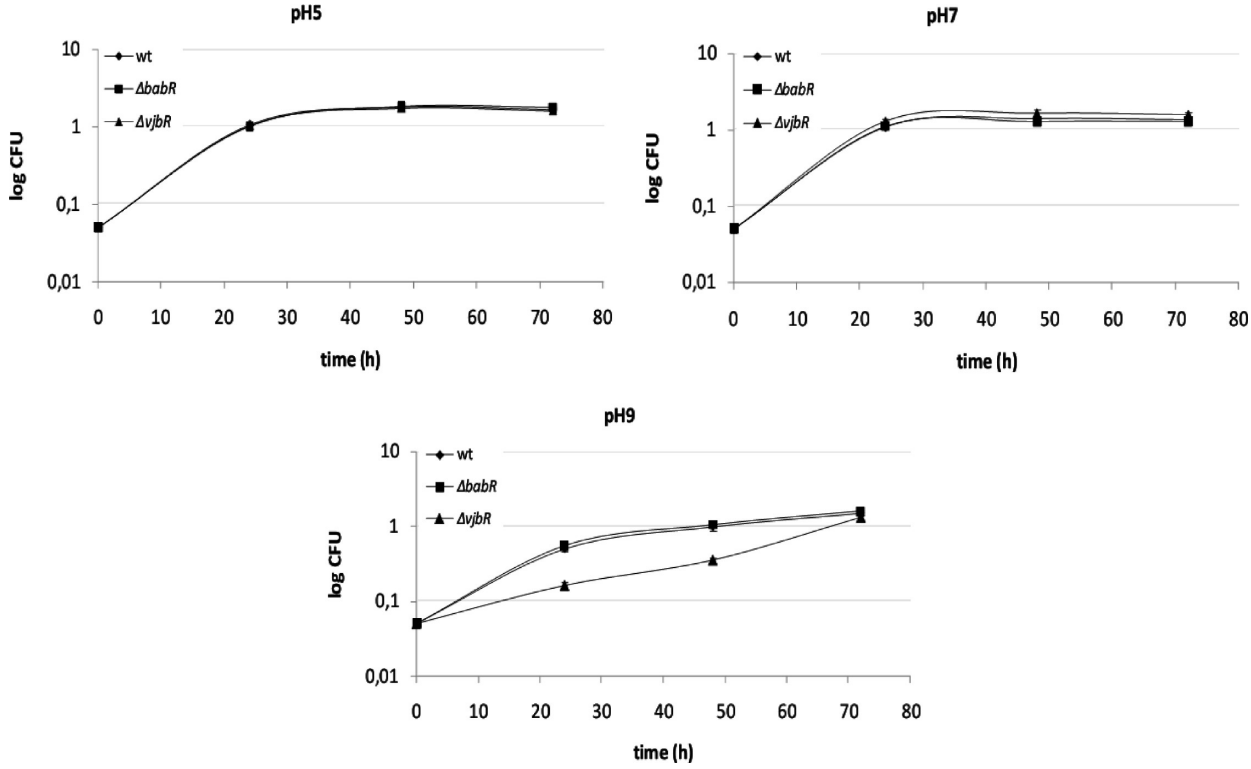

Figure 3. *B. melitensis* wt, Δ*vjbR* and Δ*babR* response to acid and alkaline stresses. Strains were growth in 2YT pH 5, 7, or 9 and CFU were compared with cultures in 2YT (100% of survival). Error bars represent standard deviation from three independent experiments. CFU, colony forming unit.

environmental stress and changes in metabolite concentrations and that was described as being crucial both for stationary phase survival and infection in murine model.[53] An additional interesting observation resulting from the analysis of the VjbR transcriptomic data is the presence of Bru-RS1 sequences near several VjbR targets. Bru-RS1 are conserved palindromic DNA sequences of 103 bp.[54] Their function is still unknown, but 30% of the 41 full length Bru-RS1 detected in the *B. melitensis* 16 M genome are located upstream (2/12 Bru-RS1) or downstream (10/12 Bru-RS1) of VjbR targets, and all of these genes are repressed by this regulator. We propose that these Bru-RS, when transcribed, could act as regulatory RNAs in conjunction with the Hfq protein, whose gene is also repressed by VjbR. The involvement of sRNA in QS regulatory systems is widespread[55,56] and often allows a supplementary level of control on QS targets in response to environmental conditions.[57,58]

In general, genes involved in DNA replication and transcription appeared to be activated by BabR and repressed by VjbR in *B. melitensis* 16 M.

Identification of Direct VjbR Targets Using Chromatin Immunoprecipitation. The proteomic and transcriptomic approaches used in the study are complementary, but lead to the identification of both direct and indirect targets. The identification of the DNA binding sites recognized by VjbR and BabR would allow the subsequent identification of the whole direct regulon of *Brucella* QS regulators. Given the involvement of VjbR in *B. melitensis* virulence, we focused on the identification of direct targets of VjbR using a chromatin immunoprecipitation assay (ChIP), a technique allowing the detection of protein−DNA interactions *in vivo*. In order to be able to detect a direct binding between VjbR and a target promoter, we used a strain expressing a constitutive VjbR regulator (unresponsive to AHLs). Specifically, the Δ*vjbR*/pSB502 strain expresses the $vjbR_{HTH}$-FLAG allele coding for the helix turn helix domain of VjbR fused with a C-terminal FLAG tag,[28] under the control of the *E. coli lac* promoter (P*lac*) in a *vjbR* deficient background. As VjbR is essential for the expression of the *virB* operon, we verified that the Δ*vjbR*/pSB502 strain produces the VirB8 protein, indicating the functionality of the $VjbR_{HTH}$-FLAG regulator (data not shown). The immunoprecipitation experiments were performed in parallel with the Δ*vjbR*/pSB502 (Δ*vjbR*, P*lac*-$vjbR_{HTH}$-FLAG) and the Δ*vjbR* strain harboring the empty plasmid (pBBR1-MCS5) as a negative control. Real-Time PCR was then used to quantify upstream regions of the targets displaying the highest ratios observed by the transcriptomic analysis and we performed RT-PCR to quantify the immunoprecipitated upstream regions.

Figure 4 illustrates ChIP analysis showing an enrichment of target genes in the $VjbR_{HTH}$-FLAG immunoprecipitation compared to the control immunoprecipitation (nontagged strain). Given that the DNA was sonicated to obtain fragments with an average size of 500 bp, these results suggest that VjbR is able to bind to the promoter region of *virB* operon, *omp25b* (BMEI1007), *omp36* (BMEI1305), BMEI0668 coding for a putative calcium binding protein, BMEI0030 coding for a hypothetical protein conserved in *P. aeruginosa* (36% of identity, 60% of similarity), and BMEII0590 and BMEII0734 both encoding for components of ABC transporters (specific for sugars and oligopeptides, respectively). Interestingly, three regions of the *virB1-virB2* locus seem to be bound by VjbR. The first one (locus 1 on the top of figure 2) corresponds to the previously defined P*virB* promoter.[59] The other two correspond to the *virB1-virB2* intergenic region (435 bp). The group of Sieira et al. has demonstrated by primer extension that *virB* transcription starts at a unique site, however the *virB1-virB2* intergenic region also seems to include regulatory site(s).[59] This proposition has been recently confirmed by the study of de Jong and collaborators[36] where the authors demonstrated by EMSA that VjbR is able to bind both the *B. abortus* P*virB* and *virB1-virB2* intergenic regions. Our ChIP experiment demonstrated that in *B. melitensis*, VjbR was also able to bind these regions *in vivo*.

In an attempt to find the DNA motif recognized by VjbR, we analyzed the upstream regions of genes directly bound by VjbR using the RSAT web resource[60] and the MEME motif discovery tool,[61] without success.

Among the 144 genes predicted to be under the control of a consensus *virB* promoter box in *B. abortus*,[36] we found only 10 of their *B. melitensis* homologues in our screens (Table 2). However, the consensus *virB* promoter VjbR box defined in the study of de Jong[36] was found in only 3 promoter sequences of the 8 VjbR targets found in our ChIP analysis (BMEI1007, BMEII0025 and BMEII0026). This observation suggests that the VjbR binding site is not well-conserved or is not present in all promoters that are direct targets of VjbR.

Conclusions

Our study is the first report of the impact of QS at the genome scale in an intracellular pathogen. *Brucella* QS was initially discovered through its impact on virulence both in cellular and mouse models,[19] and the present study confirms that QS regulates numerous genes previously identified as being essential for the full virulence of *Brucella* (Supplementary Table 2, Supporting Information). Nevertheless, the main conclusion of this paper is that QS should not be considered anymore only as a virulence regulatory system, but should also be viewed as a major global coordinator of crucial cellular and metabolic processes related to the adaptation of *Brucella* to its intracellular niche.

Indeed, the proteomic and transcriptomic analyses of the *B. melitensis* QS mutants showed that genes whose products are predicted to perform the following function are regulated by QS: (i) response to oxidative stress (*sodC, hfq*...), (ii) general stress response and protein folding (*groES, groEL*...), (iii) respiration under aerobic conditions (*coxA, coxB, coxC*), (iv) response to varied nutrients availability (sugar and amino acid transporters...), (v) enzymes of the glycolytic and TCA pathway and (vi) numerous ribosomal proteins. These observations are in agreement with previous claims that *Brucella* strains meet nutritionally poor and microaerobic environments during their infectious cycle[50,62] and that they engage an adaptive response by quantitative reduction of cellular processes participating in energy, protein, and nucleic acid metabolism.[63]

We propose that VjbR is required early in host cell infection not only to activate the genes encoding the T4SS (necessary to reach the permissive replicative-compartment)[35] but also for the early adaptation of *B. melitensis* 16 M to the stressful conditions encountered in the vacuole and in the slowdown of this strain's basic metabolism. This would prevent multiplication until the replicative compartment is reached. This proposal is well supported by the recent kinetic analysis of the *B. abortus* proteome during macrophage infection.[17] After an initial shut down of the intracellular *Brucellae*'s basic cellular processes in the early steps of macrophage infection, a majority of these proteins return to their initial level later during the infection. We propose that BabR could be a player in this latter step since it acts in an opposite way compared to VjbR on

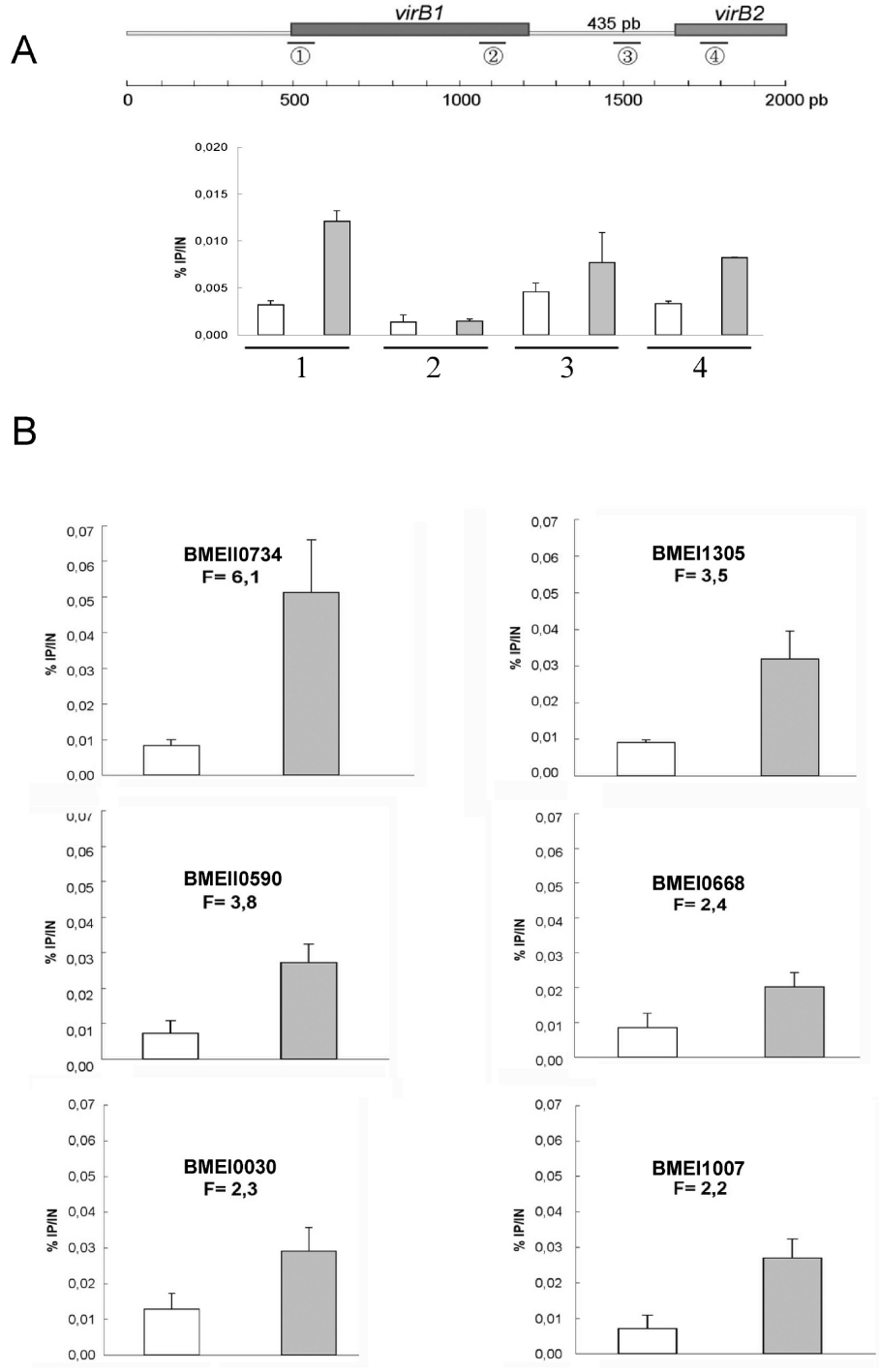

Figure 4. ChIP experiments showing direct binding of VjbR on several promoter regions. (A) Detection of several *virB1-virB2* regions. (B) Detection of BMEII0734, BMEII0590, BMEI0030, BMEI1305, BMEI0668 and BMEI1007 promoter regions. All ChIP were performed with a C-terminal Flag-tagged VjbR-HTH protein expressed from a high copy plasmid (pSB502). The *y*-axis represents the ratio of immunoprecipited product (IP) versus input (IN) (%IP/IN). White columns represent IP from control strain (Δ*vjbR*, empty plasmid), gray columns represent IP from (Δ*vjbR*, pSB502). Error bars represent standard deviation from three independent experiments.

several key QS targets including the genes encoding the VirB proteins, GroESL and key central metabolic enzymes.

Particularly striking also is the parallelism that can be drawn between the targets identified as part of the QS regulon in this study and the direct or indirect targets of another major regulator of *Brucella* virulence: the two component system (TCS) BvrS/BvrR. The results presented here, along with those from a previous study[28] strongly support the involvement of VjbR in the control of envelope properties in *Brucella* strains, and this appears also to be the case for BvrS/BvrR.[64−66] More importantly, a recent proteomic analysis of outer membrane fragments released by *B. abortus bvrR*/*bvrS* mutants[67] pointed out an important increase of periplasmic proteins, ABC transporters and chaperones in these mutants compared to the parent strain. The expression of genes encoding products belonging to these same functional categories are also clearly

increased in our v*jbR* mutant (see Table 2A, E). In both the *bvrS/R* mutants and in the *vjbR* mutant, these kinds of changes seem to mimic nutrient starvation. Consequently, BvrS/BvrR was suggested to be directly or indirectly involved in adjusting the metabolism of *Brucella*[67] and, considering the impact of the QS system on central metabolism (see Table 2B), a similar proposition can be clearly put forth for this latter system. However, neither the analysis of Lamontagne[67] nor our analyses have demonstrated a link between the BvrS/BvrR system and VjbR. Nevertheless, these analyses have been performed under very dissimilar conditions and we cannot exclude the possibility that these two regulatory pathways could be connected (directly or indirectly through other global starvation sensing mechanisms like the stringent response[68] and/or the PTS system[18]). Altogether, these systems should contribute to the adaptation of the metabolic network during the nutrient shift faced by *Brucella* all along its intracellular trafficking.

In summary, our results demonstrate that *B. melitensis* 16 M possesses a nonclassical QS regulatory system since: (i) despite the lack of a classical AHL-synthase in this pathogen, QS regulates a large fraction of its genome under the conditions tested, (ii) BabR can behave as a modulator of VjbR activity, (iii) C_{12}−HSL have an effect both on BabR and VjbR, and (iv) QS is involved in the intracellular survival of *B. melitensis* through VjbR.

The use of a QS system in the individual vacuole surrounding the *Brucellae* in the host cell represents a good example of "efficiency sensing", in agreement with the definition of Hense and co-workers,[25] since the diffusion of AHLs in these compartments should be delayed compared to the environments encountered by these bacteria before their entry into host cells. This proposal and the biosynthetic pathway responsible of the production of low amounts of C_{12}−HSL[32] should be further investigated to get further insights on QS in *Brucella* strains.

Abbrevations: 3PG, 3-P-glycerate; AA, amino acid; AcoA, acetyl coenzyme A; AHL, acyl-homoserine lactone; BCV, *Brucella* containing vacuole; CDS, coding sequence; CFU, colony forming unit; ChIP, chromatin immunoprecipitation; DNA, DNA; EPS, exopolysaccharide; ER, endoplasmic reticulum; F6P, fructose-6-P; FC, fold change; Ga3P, glyceraldehyde-3-P; G1P, glycerol-1-P; GLU, glutamate; Gnt, gentamycin; HTH, helix-turn-helix; ISO, isocitrate; LPS, lipopolysaccharide; MacP, malonyl acyl carrier protein; McoA, malonyl coenzyme A; Nal, nalidixic acid; OMP, outer membrane protein; OXA, oxaloacetate; Pentose-P, pentose phosphate pathway; PYR, pyruvate; QS, Quorum Sensing; RNA, ribonucleic acid; SUC, succinate; T4SS, type four secretion system; TCS, two component system; TCA, tricarboxylic acid cycle; wt, wild type.

Acknowledgment. We thank past and present members of the *Brucella* team of the URBM for fruitful discussions and R. Martin Roop, II for critical reading of the manuscript and for improving the English. This work was supported by the Commission of the European Communities (contract no. QLK2-CT-1999-00014), the FRFC (Fonds de la Recherche Fondamentale Collective, conventions 2.4521.04 and 2.4521.08), and the ARC fellowship (Actions de Recherches Concertées, conventions 04/09-325 and 08/13-015). S.U. and J.L. hold a specialization grant from the Fonds pour la Formation à la Recherche dans l'Industrie et l'Agriculture (FRIA).

Supporting Information Available: Supplementary Tables 1−3. This material is available free of charge via the Internet at http://pubs.acs.org.

References

(1) Pappas, G.; Papadimitriou, P.; Akritidis, N.; Christou, L.; Tsianos, E. V. The new global map of human brucellosis. *Lancet Infect. Dis.* **2006**, *6* (2), 91–9.
(2) Smith, L. D.; Ficht, T. A. Pathogenesis of *Brucella*. *Crit. Rev. Microbiol.* **1990**, *17* (3), 209–30.
(3) Corbel, M. J. Brucellosis: an overview. *Emerg Infect. Dis.* **1997**, *3* (2), 213–21.
(4) Center for Disease Control and Prevention: Select agent program. http://www.cdc.gov/od/sap.
(5) Celli, J. Surviving inside a macrophage: the many ways of. *Res. Microbiol.* **2006**, *157* (2), 93–8.
(6) Detilleux, P. G.; Deyoe, B. L.; Cheville, N. F. Penetration and intracellular growth of *Brucella abortus* in nonphagocytic cells in vitro. *Infect. Immun.* **1990**, *58* (7), 2320–8.
(7) Ficht, T. A. Intracellular survival of *Brucella*: defining the link with persistence. *Vet. Microbiol.* **2003**, *92* (3), 213–23.
(8) Pizarro-Cerda, J.; Meresse, S.; Parton, R. G.; van der Goot, G.; Sola-Landa, A.; Lopez-Goni, I.; Moreno, E.; Gorvel, J. P. Brucella abortus transits through the autophagic pathway and replicates in the endoplasmic reticulum of nonprofessional phagocytes. *Infect. Immun.* **1998**, *66* (12), 5711–24.
(9) Barquero-Calvo, E.; Chaves-Olarte, E.; Weiss, D. S.; Guzman-Verri, C.; Chacon-Diaz, C.; Rucavado, A.; Moriyon, I.; Moreno, E. Brucella abortus uses a stealthy strategy to avoid activation of the innate immune system during the onset of infection. *PLoS ONE* **2007**, *2*, e631.
(10) Starr, T.; Ng, T. W.; Wehrly, T. D.; Knodler, L. A.; Celli, J. Brucella intracellular replication requires trafficking through the late endosomal/lysosomal compartment. *Traffic* **2008**, *9* (5), 678–94.
(11) Moreno, E.; Moriyon, I. The genus *Brucella*. In *The prokaryotes. Electronic version.*; Dworkin, M., Falkow, S., Rosenberg, E., Schleifer, K.-H., Stackebrandt, E., Eds.; Springer: New York, 2001.
(12) Kohler, S.; Foulongne, V.; Ouahrani-Bettache, S.; Bourg, G.; Teyssier, J.; Ramuz, M.; Liautard, J. P. The analysis of the intramacrophagic virulome of *Brucella suis* deciphers the environment encountered by the pathogen inside the macrophage host cell. *Proc. Natl. Acad. Sci. U.S.A.* **2002**, *99* (24), 15711–6.
(13) Roop, R. M., 2nd; Bellaire, B. H.; Valderas, M. W.; Cardelli, J. A. Adaptation of the *Brucellae* to their intracellular niche. *Mol. Microbiol.* **2004**, *52* (3), 621–30.
(14) Porte, F.; Liautard, J. P.; Kohler, S. Early acidification of phagosomes containing *Brucella suis* is essential for intracellular survival in murine macrophages. *Infect. Immun.* **1999**, *67* (8), 4041–7.
(15) Kohler, S.; Michaux-Charachon, S.; Porte, F.; Ramuz, M.; Liautard, J. P. What is the nature of the replicative niche of a stealthy bug named *Brucella*. *Trends Microbiol* **2003**, *11* (5), 215–9.
(16) Kohler, S.; Porte, F.; Jubier-Maurin, V.; Ouahrani-Bettache, S.; Teyssier, J.; Liautard, J. P. The intramacrophagic environment of *Brucella suis* and bacterial response. *Vet. Microbiol.* **2002**, *90* (1−4), 299–309.
(17) Lamontagne, J.; Forest, A.; Marazzo, E.; Denis, F.; Butler, H.; Michaud, J. F.; Boucher, L.; Pedro, I.; Villeneuve, A.; Sitnikov, D.; Trudel, K.; Nassif, N.; Boudjelti, D.; Tomaki, F.; Chaves-Olarte, E.; Guzman-Verri, C.; Brunet, S.; Cote-Martin, A.; Hunter, J.; Moreno, E.; Paramithiotis, E. Intracellular Adaptation of *Brucella abortus*. *J. Proteome Res.* **2009**, *8* (3), 1594–609.
(18) Letesson, J. J.a. D. B., X., *Brucella - Molecular and Cellular Biology*; Horizon Bioscience: Norfolk, 2004; pp 117−58.
(19) Delrue, R. M.; Deschamps, C.; Leonard, S.; Nijskens, C.; Danese, I.; Schaus, J. M.; Bonnot, S.; Ferooz, J.; Tibor, A.; De Bolle, X.; Letesson, J. J. A quorum-sensing regulator controls expression of both the type IV secretion system and the flagellar apparatus of *Brucella melitensis*. *Cell Microbiol.* **2005**, *7* (8), 1151–61.
(20) Sjoblom, S.; Brader, G.; Koch, G.; Palva, E. T. Cooperation of two distinct ExpR regulators controls quorum sensing specificity and virulence in the plant pathogen *Erwinia carotovora*. *Mol. Microbiol.* **2006**, *60* (6), 1474–89.
(21) Smith, R. S.; Iglewski, B. H. *P. aeruginosa* quorum-sensing systems and virulence. *Curr. Opin. Microbiol.* **2003**, *6* (1), 56–60.
(22) Waters, C. M.; Bassler, B. L. Quorum Sensing: Cell-to-Cell Communication in Bacteria. *Annu. Rev. Cell Dev. Biol.* **2005**, *21*, 319–46.
(23) Hastings, J. W.; Nealson, K. H. Bacterial bioluminescence. *Annu. Rev. Microbiol.* **1977**, *31*, 549–95.

(24) Fuqua, W. C.; Winans, S. C.; Greenberg, E. P. Quorum sensing in bacteria: the LuxR-LuxI family of cell density-responsive transcriptional regulators. *J. Bacteriol.* **1994**, *176* (2), 269–75.
(25) Hense, B. A.; Kuttler, C.; Muller, J.; Rothballer, M.; Hartmann, A.; Kreft, J. U. Does efficiency sensing unify diffusion and quorum sensing. *Nat. Rev. Microbiol.* **2007**, *5* (3), 230–9.
(26) Redfield, R. J. Is quorum sensing a side effect of diffusion sensing. *Trends Microbiol.* **2002**, *10* (8), 365–70.
(27) DelVecchio, V. G.; Kapatral, V.; Redkar, R. J.; Patra, G.; Mujer, C.; Los, T.; Ivanova, N.; Anderson, I.; Bhattacharyya, A.; Lykidis, A.; Reznik, G.; Jablonski, L.; Larsen, N.; D'Souza, M.; Bernal, A.; Mazur, M.; Goltsman, E.; Selkov, E.; Elzer, P. H.; Hagius, S.; O'Callaghan, D.; Letesson, J. J.; Haselkorn, R.; Kyrpides, N.; Overbeek, R. The genome sequence of the facultative intracellular pathogen *Brucella melitensis*. *Proc. Natl. Acad. Sci. U.S.A.* **2002**, *99* (1), 443–8.
(28) Uzureau, S.; Godefroid, M.; Deschamps, C.; Lemaire, J.; De Bolle, X.; Letesson, J. J. Mutations of the Quorum Sensing-dependent regulator VjbR lead to drastic surface modifications in *Brucella melitensis*. *J. Bacteriol.* **2007**, *189*, 6035–47.
(29) Letesson, J. J.; Lestrate, P.; Delrue, R. M.; Danese, I.; Bellefontaine, F.; Fretin, D.; Taminiau, B.; Tibor, A.; Dricot, A.; Deschamps, C.; Haine, V.; Leonard, S.; Laurent, T.; Mertens, P.; Vandenhaute, J.; De Bolle, X. Fun stories about *Brucella*: the "furtive nasty bug". *Vet. Microbiol.* **2002**, *90* (1−4), 317–28.
(30) Rambow-Larsen, A. A.; Rajashekara, G.; Petersen, E.; Splitter, G. Putative quorum-sensing regulator BlxR of *Brucella melitensis* regulates virulence factors including the type IV secretion system and flagella. *J. Bacteriol.* **2008**, *190* (9), 3274–82.
(31) Taminiau, B., Etude du Quorum Sensing chez *Brucella melitensis* 16 M. Thesis, ISBN: 2-87037-399-6, 2003.
(32) Taminiau, B.; Daykin, M.; Swift, S.; Boschiroli, M. L.; Tibor, A.; Lestrate, P.; De Bolle, X.; O'Callaghan, D.; Williams, P.; Letesson, J. J. Identification of a quorum-sensing signal molecule in the facultative intracellular pathogen *Brucella melitensis*. *Infect. Immun.* **2002**, *70* (6), 3004–11.
(33) Delrue, R., Contribution à l'analyse des mécanismes moléculaires impliqués dans le traffic intracellulaire de *Brucella melitensis* 16 M. Thesis, ISBN: 2−87037−372−4, 2002.
(34) Fretin, D.; Fauconnier, A.; Kohler, S.; Halling, S.; Leonard, S.; Nijskens, C.; Ferooz, J.; Lestrate, P.; Delrue, R. M.; Danese, I.; Vandenhaute, J.; Tibor, A.; DeBolle, X.; Letesson, J. J. The sheathed flagellum of *Brucella melitensis* is involved in persistence in a murine model of infection. *Cell Microbiol.* **2005**, *7* (5), 687–98.
(35) Comerci, D. J.; Martinez-Lorenzo, M. J.; Sieira, R.; Gorvel, J. P.; Ugalde, R. A. Essential role of the VirB machinery in the maturation of the *Brucella abortus*-containing vacuole. *Cell Microbiol.* **2001**, *3* (3), 159–68.
(36) de Jong, M. F.; Sun, Y. H.; den Hartigh, A. B.; van Dijl, J. M.; Tsolis, R. M. Identification of VceA and VceC, two members of the VjbR regulon that are translocated into macrophages by the *Brucella* type IV secretion system. *Mol. Microbiol.* **2008**, *70* (6), 1378–96.
(37) Kovach, M. E.; Elzer, P. H.; Hill, D. S.; Robertson, G. T.; Farris, M. A.; Roop, R. M.; Peterson, K. M. Four new derivatives of the broad-host-range cloning vector pBBR1MCS, carrying different antibiotic-resistance cassettes. *Gene* **1995**, *166* (1), 175–6.
(38) Dricot, A.; Rual, J. F.; Lamesch, P.; Bertin, N.; Dupuy, D.; Hao, T.; Lambert, C.; Hallez, R.; Delroisse, J. M.; Vandenhaute, J.; Lopez-Goni, I.; Moriyon, I.; Garcia-Lobo, J. M.; Sangari, F. J.; Macmillan, A. P.; Cutler, S. J.; Whatmore, A. M.; Bozak, S.; Sequerra, R.; Doucette-Stamm, L.; Vidal, M.; Hill, D. E.; Letesson, J. J.; De Bolle, X. Generation of the *Brucella melitensis* ORFeome version 1.1. *Genome Res.* **2004**, *14* (10B), 2201–6.
(39) Berger, F. D.; H, B.; Pierre, M.; Gaigneaux, A.; Depiereux, E. The "Window t-test": a simple and powerful approach to detect differentially expressed genes in microarray datasets. *Cent. Eur. J. Biol.* **2008**, *3* (3), 327–344.
(40) Irizarry, R. A.; Hobbs, B.; Collin, F.; Beazer-Barclay, Y. D.; Antonellis, K. J.; Scherf, U.; Speed, T. P. Exploration, normalization, and summaries of high density oligonucleotide array probe level data. *Biostatistics* **2003**, *4* (2), 249–64.
(41) Lamanda, A.; Zahn, A.; Roder, D.; Langen, H. Improved Ruthenium II tris (bathophenantroline disulfonate) staining and destaining protocol for a better signal-to-background ratio and improved baseline resolution. *Proteomics* **2004**, *4* (3), 599–608.
(42) Shevchenko, A.; Wilm, M.; Vorm, O.; Mann, M. Mass spectrometric sequencing of proteins silver-stained polyacrylamide gels. *Anal. Chem.* **1996**, *68* (5), 850–8.
(43) Kuras, L.; Struhl, K. Binding of TBP to promoters *in vivo* is stimulated by activators and requires Pol II holoenzyme. *Nature* **1999**, *399* (6736), 609–13.
(44) DeLisa, M. P.; Wu, C. F.; Wang, L.; Valdes, J. J.; Bentley, W. E. DNA microarray-based identification of genes controlled by autoinducer 2-stimulated quorum sensing in Escherichia coli. *J. Bacteriol.* **2001**, *183* (18), 5239–47.
(45) Schuster, M.; Lostroh, C. P.; Ogi, T.; Greenberg, E. P. Identification, timing, and signal specificity of *Pseudomonas aeruginosa* quorum-controlled genes: a transcriptome analysis. *J. Bacteriol.* **2003**, *185* (7), 2066–79.
(46) Wagner, V. E.; Bushnell, D.; Passador, L.; Brooks, A. I.; Iglewski, B. H. Microarray analysis of *Pseudomonas aeruginosa* quorum-sensing regulons: effects of growth phase and environment. *J. Bacteriol.* **2003**, *185* (7), 2080–95.
(47) Wagner, V. E.; Gillis, R. J.; Iglewski, B. H. Transcriptome analysis of quorum-sensing regulation and virulence factor expression in *Pseudomonas aeruginosa*. *Vaccine* **2004**, *22* (Suppl 1), S15–20.
(48) Delpino, M. V.; Marchesini, M. I.; Estein, S. M.; Comerci, D. J.; Cassataro, J.; Fossati, C. A.; Baldi, P. C. A bile salt hydrolase of *Brucella abortus* contributes to the establishment of a successful infection through the oral route in mice. *Infect. Immun.* **2007**, *75* (1), 299–305.
(49) Delpino, M. V.; Comerci, D. J.; Wagner, M. A.; Eschenbrenner, M.; Mujer, C. V.; Ugalde, R. A.; Fossati, C. A.; Baldi, P. C.; Delvecchio, V. G. Differential composition of culture supernatants from wild-type *Brucella abortus* and its isogenic *virB* mutants. *Arch. Microbiol.* **2009**, *191* (7), 571–81.
(50) Kohler, S.; Ekaza, E.; Paquet, J. Y.; Walravens, K.; Teyssier, J.; Godfroid, J.; Liautard, J. P. Induction of *dnaK* through its native heat shock promoter is necessary for intramacrophagic replication of Brucella suis. *Infect. Immun.* **2002**, *70* (3), 1631–4.
(51) Appelbe, O. K.; Sedgley, C. M. Effects of prolonged exposure to alkaline pH on *Enterococcus faecalis* survival and specific gene transcripts. *Oral Microbiol. Immunol.* **2007**, *22* (3), 169–74.
(52) Hallez, R.; Mignolet, J.; Van Mullem, V.; Wery, M.; Vandenhaute, J.; Letesson, J. J.; Jacobs-Wagner, C.; De Bolle, X. The asymmetric distribution of the essential histidine kinase PdhS indicates a differentiation event in *Brucella abortus*. *Embo J.* **2007**, *26* (5), 1444–55.
(53) Robertson, G. T.; Roop, R. M., Jr. The *Brucella abortus* host factor I (HF-I) protein contributes to stress resistance during stationary phase and is a major determinant of virulence in mice. *Mol. Microbiol.* **1999**, *34* (4), 690–700.
(54) Halling, S. M.; Bricker, B. J. Characterization and occurrence of two repeated palindromic DNA elements of *Brucella spp.*: Bru-RS1 and Bru-RS2. *Mol. Microbiol.* **1994**, *14* (4), 681–9.
(55) Hammer, B. K.; Bassler, B. L. Regulatory small RNAs circumvent the conventional quorum sensing pathway in pandemic *Vibrio cholerae*. *Proc. Natl. Acad. Sci. U.S.A.* **2007**, *104* (27), 11145–9.
(56) Novick, R. P.; Ross, H. F.; Projan, S. J.; Kornblum, J.; Kreiswirth, B.; Moghazeh, S. Synthesis of staphylococcal virulence factors is controlled by a regulatory RNA molecule. *Embo J.* **1993**, *12* (10), 3967–75.
(57) Bejerano-Sagie, M.; Xavier, K. B. The role of small RNAs in quorum sensing. *Curr. Opin. Microbiol.* **2007**, *10* (2), 189–98.
(58) Toledo-Arana, A.; Repoila, F.; Cossart, P. Small noncoding RNAs controlling pathogenesis. *Curr. Opin. Microbiol.* **2007**, *10* (2), 182–8.
(59) Sieira, R.; Comerci, D. J.; Pietrasanta, L. I.; Ugalde, R. A. Integration host factor is involved in transcriptional regulation of the *Brucella abortus virB* operon. *Mol. Microbiol.* **2004**, *54* (3), 808–22.
(60) van Helden, J. Regulatory sequence analysis tools. *Nucleic Acids Res.* **2003**, *31* (13), 3593–6.
(61) Bailey, T. L.; Williams, N.; Misleh, C.; Li, W. W. MEME: discovering and analyzing DNA and protein sequence motifs. *Nucleic Acids Res.* **2006**, *34* (Web Server issue), W369–73.
(62) Al Dahouk, S.; Loisel-Meyer, S.; Scholz, H. C.; Tomaso, H.; Kersten, M.; Harder, A.; Neubauer, H.; Kohler, S.; Jubier-Maurin, V. Proteomic analysis of *Brucella suis* under oxygen deficiency reveals flexibility in adaptive expression of various pathways. *Proteomics* **2009**, *9* (11), 3011–21.
(63) Al Dahouk, S.; Jubier-Maurin, V.; Scholz, H. C.; Tomaso, H.; Karges, W.; Neubauer, H.; Kohler, S. Quantitative analysis of the intramacrophagic *Brucella suis* proteome reveals metabolic adaptation to late stage of cellular infection. *Proteomics* **2008**, *8* (18), 3862–70.
(64) Guzman-Verri, C.; Manterola, L.; Sola-Landa, A.; Parra, A.; Cloeckaert, A.; Garin, J.; Gorvel, J. P.; Moriyon, I.; Moreno, E.; Lopez-Goni, I. The two-component system BvrR/BvrS essential for *Brucella abortus* virulence regulates the expression of outer membrane proteins with counterparts in members of the *Rhizobiaceae*. *Proc. Natl. Acad. Sci. U.S.A.* **2002**, *99* (19), 12375–80.

(65) Manterola, L.; Moriyon, I.; Moreno, E.; Sola-Landa, A.; Weiss, D. S.; Koch, M. H.; Howe, J.; Brandenburg, K.; Lopez-Goni, I. The lipopolysaccharide of *Brucella abortus* BvrS/BvrR mutants contains lipid A modifications and has higher affinity for bactericidal cationic peptides. *J. Bacteriol.* **2005**, *187* (16), 5631–9.
(66) Sola-Landa, A.; Pizarro-Cerda, J.; Grillo, M. J.; Moreno, E.; Moriyon, I.; Blasco, J. M.; Gorvel, J. P.; Lopez-Goni, I. A two-component regulatory system playing a critical role in plant pathogens and endosymbionts is present in *Brucella abortus* and controls cell invasion and virulence. *Mol. Microbiol.* **1998**, *29* (1), 125–38.
(67) Lamontagne, J.; Butler, H.; Chaves-Olarte, E.; Hunter, J.; Schirm, M.; Paquet, C.; Tian, M.; Kearney, P.; Hamaidi, L.; Chelsky, D.; Moriyon, I.; Moreno, E.; Paramithiotis, E. Extensive cell envelope modulation is associated with virulence in *Brucella abortus*. *J. Proteome Res.* **2007**, *6* (4), 1519–29.
(68) Dozot, M.; Boigegrain, R. A.; Delrue, R. M.; Hallez, R.; Ouahrani-Bettache, S.; Danese, I.; Letesson, J. J.; De Bolle, X.; Kohler, S. The stringent response mediator Rsh is required for *Brucella melitensis* and *Brucella suis* virulence, and for expression of the type IV secretion system virB. *Cell Microbiol.* **20068**, (11), 1791–802.
(69) Kohler, S.; Ouahrani-Bettache, S.; Layssac, M.; Teyssier, J.; Liautard, J. P. Constitutive and inducible expression of green fluorescent protein in *Brucella suis*. *Infect. Immun.* **1999**, *67* (12), 6695–7.
(70) Foulongne, V.; Bourg, G.; Cazevieille, C.; Michaux-Charachon, S.; O'Callaghan, D. Identification of *Brucella suis* genes affecting intracellular survival in an in vitro human macrophage infection model by signature-tagged transposon mutagenesis. *Infect. Immun.* **2000**, *68* (3), 1297–303.
(71) Kim, S.; Watarai, M.; Kondo, Y.; Erdenebaatar, J.; Makino, S.; Shirahata, T. Isolation and characterization of mini-Tn5Km2 insertion mutants of *Brucella abortus* deficient in internalization and intracellular growth in HeLa cells. *Infect. Immun.* **2003**, *71* (6), 3020–7.
(72) Hong, P. C.; Tsolis, R. M.; Ficht, T. A. Identification of genes required for chronic persistence of *Brucella abortus* in mice. *Infect. Immun.* **2000**, *68* (7), 4102–7.
(73) Allen, C. A.; Adams, L. G.; Ficht, T. A. Transposon-derived *Brucella abortus* rough mutants are attenuated and exhibit reduced intracellular survival. *Infect. Immun.* **1998**, *66* (3), 1008–16.
(74) Kohler, S.; Teyssier, J.; Cloeckaert, A.; Rouot, B.; Liautard, J. P. Participation of the molecular chaperone DnaK in intracellular growth of *Brucella suis* within U937-derived phagocytes. *Mol. Microbiol.* **1996**, *20* (4), 701–12.
(75) Tibor, A.; Wansard, V.; Bielartz, V.; Delrue, R. M.; Danese, I.; Michel, P.; Walravens, K.; Godfroid, J.; Letesson, J. J. Effect of omp10 or omp19 deletion on *Brucella abortus* outer membrane properties and virulence in mice. *Infect. Immun.* **2002**, *70* (10), 5540–6.
(76) Delrue, R. M.; Martinez-Lorenzo, M.; Lestrate, P.; Danese, I.; Bielarz, V.; Mertens, P.; De Bolle, X.; Tibor, A.; Gorvel, J. P.; Letesson, J. J. Identification of *Brucella spp.* genes involved in intracellular trafficking. *Cell Microbiol.* **2001**, *3* (7), 487–97.
(77) O'Callaghan, D.; Cazevieille, C.; Allardet-Servent, A.; Boschiroli, M. L.; Bourg, G.; Foulongne, V.; Frutos, P.; Kulakov, Y.; Ramuz, M. A homologue of the *Agrobacterium tumefaciens* VirB and *Bordetella pertussis* Ptl type IV secretion systems is essential for intracellular survival of *Brucella suis*. *Mol. Microbiol.* **1999**, *33* (6), 1210–20.
(78) Sieira, R.; Comerci, D. J.; Sanchez, D. O.; Ugalde, R. A. A homologue of an operon required for DNA transfer in *Agrobacterium* is required in *Brucella abortus* for virulence and intracellular multiplication. *J. Bacteriol.* **2000**, *182* (17), 4849–55.
(79) Latimer, E.; Simmers, J.; Sriranganathan, N.; Roop, R. M., 2nd; Schurig, G. G.; Boyle, S. M. *Brucella abortus* deficient in copper/zinc superoxide dismutase is virulent in BALB/c mice. *Microb. Pathog.* **1992**, *12* (2), 105–13.
(80) Lestrate, P.; Dricot, A.; Delrue, R. M.; Lambert, C.; Martinelli, V.; De Bolle, X.; Letesson, J. J.; Tibor, A. Attenuated signature-tagged mutagenesis mutants of *Brucella melitensis* identified during the acute phase of infection in mice. *Infect. Immun.* **2003**, *71* (12), 7053–60.

PR100068P